

- lysine methyltransferase G9a and histone deacetylase 1. *Mol Cell Biol* 25: 10338–10351.
24. Zhu J, Guo L, Min B, Watson CJ, Hu-Li J, et al. (2002) Growth factor independent-1 induced by IL-4 regulates Th2 cell proliferation. *Immunity* 16: 733–744.
 25. Shinnakasu R, Yamashita M, Kuwahara M, Hosokawa H, Hasegawa A, et al. (2008) Gfi1-mediated stabilization of GATA3 protein is required for Th2 cell differentiation. *J Biol Chem* 283: 28216–28225.
 26. Northrup DL, Zhao K (2011) Application of ChIP-Seq and related techniques to the study of immune function. *Immunity* 34: 830–842.
 27. Bannister AJ, Kouzarides T (2011) Regulation of chromatin by histone modifications. *Cell Res* 21: 381–395.
 28. Agarwal S, Avni O, Rao A (2000) Cell-type-restricted binding of the transcription factor NFAT to a distal IL-4 enhancer in vivo. *Immunity* 12: 643–652.
 29. Tanaka S, Motomura Y, Suzuki Y, Yagi R, Inoue H, et al. (2011) The enhancer HS2 critically regulates GATA-3-mediated Il4 transcription in T(H)2 cells. *Nat Immunol* 12: 77–85.
 30. Yamashita M, Ukai-Tadenuma M, Kimura M, Omori M, Inami M, et al. (2002) Identification of a conserved GATA3 response element upstream proximal from the interleukin-13 gene locus. *J Biol Chem* 277: 42399–42408.
 31. Lee GR, Spilianakis CG, Flavell RA (2005) Hypersensitive site 7 of the TH2 locus control region is essential for expressing TH2 cytokine genes and for long-range intra-chromosomal interactions. *Nat Immunol* 6: 42–48.
 32. Lee GR, Fields PE, Griffin TJ, Flavell RA (2003) Regulation of the Th2 cytokine locus by a locus control region. *Immunity* 19: 145–153.
 33. Schwenger GT, Fournier R, Kok CC, Mordvinov VA, Yeoman D, et al. (2001) GATA-3 has dual regulatory functions in human interleukin-5 transcription. *J Biol Chem* 276: 48502–48509.
 34. Abonia JP, Putnam PE (2011) Mepolizumab in eosinophilic disorders. *Expert Rev Clin Immunol* 7: 411–417.
 35. Haldar P, Brightling CE, Hargadon B, Gupta S, Monteiro W, et al. (2009) Mepolizumab and exacerbations of refractory eosinophilic asthma. *N Engl J Med* 360: 973–984.
 36. Hurst SD, Muchamuel T, Gorman DM, Gilbert JM, Clifford T, et al. (2002) New IL-17 family members promote Th1 or Th2 responses in the lung: in vivo function of the novel cytokine IL-25. *J Immunol* 169: 443–453.
 37. Ballantyne SJ, Barlow JL, Jolin HE, Nath P, Williams AS, et al. (2007) Blocking IL-25 prevents airway hyperresponsiveness in allergic asthma. *J Allergy Clin Immunol* 120: 1324–1331.
 38. Terashima A, Watarai H, Inoue S, Sekine E, Nakagawa R, et al. (2008) A novel subset of mouse NKT cells bearing the IL-17 receptor B responds to IL-25 and contributes to airway hyperreactivity. *J Exp Med* 205: 2727–2733.
 39. Yamashita M, Shiinakasu R, Asou H, Kimura M, Hasegawa A, et al. (2005) Ras-ERK MAPK cascade regulates GATA3 stability and Th2 differentiation through ubiquitin-proteasome pathway. *J Biol Chem* 280: 29409–29419.
 40. Ito K, Caramori G, Lim S, Oates T, Chung KF, et al. (2002) Expression and activity of histone deacetylases in human asthmatic airways. *Am J Respir Crit Care Med* 166: 392–396.
 41. Cosio BG, Mann B, Ito K, Jazrawi E, Barnes PJ, et al. (2004) Histone acetylase and deacetylase activity in alveolar macrophages and blood monocytes in asthma. *Am J Respir Crit Care Med* 170: 141–147.
 42. Khan AU, Krishnamurthy S (2005) Histone modifications as key regulators of transcription. *Front Biosci* 10: 866–872.
 43. Kuwahara M, Yamashita M, Shinoda K, Tofukuji S, Onodera A, et al. (2012) The transcription factor Sox4 is a downstream target of signaling by the cytokine TGF-beta and suppresses T(H)2 differentiation. *Nat Immunol* 13: 778–786.
 44. Yamashita M, Kuwahara M, Suzuki A, Hirahara K, Shimakasu R, et al. (2008) Bmi1 regulates memory CD4 T cell survival via repression of the Noxa gene. *J Exp Med* 205: 1109–1120.
 45. Suzuki A, Iwamura C, Shinoda K, Tumes DJ, Kimura MY, et al. (2010) Polycomb group gene product Ring1B regulates Th2-driven airway inflammation through the inhibition of Bim-mediated apoptosis of effector Th2 cells in the lung. *J Immunol* 184: 4510–4520.

Exome sequencing identifies secondary mutations of *SETBP1* and *JAK3* in juvenile myelomonocytic leukemia

Hirotochi Sakaguchi^{1,8}, Yusuke Okuno^{2,8}, Hideki Muramatsu^{1,8}, Kenichi Yoshida^{2,8}, Yuichi Shiraishi³, Mariko Takahashi², Ayana Kon², Masashi Sanada^{2,4}, Kenichi Chiba³, Hiroko Tanaka⁵, Hideki Makishima⁶, Xinan Wang¹, Yinyan Xu¹, Sayoko Doisaki¹, Asahito Hama¹, Koji Nakanishi¹, Yoshiyuki Takahashi¹, Nao Yoshida⁷, Jaroslaw P Maciejewski⁶, Satoru Miyano^{3,5}, Seishi Ogawa^{2,4,9} & Seiji Kojima^{1,9}

Juvenile myelomonocytic leukemia (JMML) is an intractable pediatric leukemia with poor prognosis¹ whose molecular pathogenesis is poorly understood, except for somatic or germline mutations of RAS pathway genes, including *PTPN11*, *NF1*, *NRAS*, *KRAS* and *CBL*, in the majority of cases^{2–4}. To obtain a complete registry of gene mutations in JMML, whole-exome sequencing was performed for paired tumor-normal DNA from 13 individuals with JMML (cases), which was followed by deep sequencing of 8 target genes in 92 tumor samples. JMML was characterized by a paucity of gene mutations (0.85 non-silent mutations per sample) with somatic or germline RAS pathway involvement in 82 cases (89%). The *SETBP1* and *JAK3* genes were among common targets for secondary mutations. Mutations in the latter were often subclonal and may be involved in the progression rather than the initiation of leukemia, and these mutations associated with poor clinical outcome. Our findings provide new insights into the pathogenesis and progression of JMML.

JMML is a rare myelodysplastic/myeloproliferative neoplasm unique to childhood, characterized by excessive proliferation of myelomonocytic cells and hypersensitivity to granulocyte-macrophage colony-stimulating factor¹. A cardinal genetic feature of JMML is frequent somatic and/or germline mutation of RAS pathway genes, such as *NF1*, *NRAS*, *KRAS*, *PTPN11* and *CBL*, which are mutated in more than 70% of JMML cases in a mutually exclusive manner^{2–4}. However, it is still open to question whether RAS pathway mutations are sufficient for the development of JMML or if secondary mutations have a role in the development and progression of this cancer. To address these issues and to better define the molecular pathogenesis of JMML, we performed whole-exome sequencing of paired tumor-normal DNA from 13 cases (Supplementary Table 1). We obtained mean coverage

in exome sequencing of 137× for tumor samples and 143× for normal samples (Supplementary Fig. 1). A Monte-Carlo simulation indicated that the study detected 88% of the existing somatic mutations (Online Methods and Supplementary Fig. 2).

Sanger sequencing of 25 candidate non-silent somatic nucleotide alterations confirmed 1 nonsense and 10 missense mutations (Table 1 and Supplementary Fig. 3), with the low true positive rate consistent with the very low numbers of somatic mutations in JMML. Of the 11 somatic mutations, 6 involved known RAS pathway genes. In addition, non-overlapping RAS pathway mutations (6 somatic and 6 germline) were confirmed in 11 of the 13 discovery cases (86%; Table 1). For the remaining two cases that lacked documented RAS pathway mutations, we intensively searched for possible germline mutations that could be relevant to the development of JMML. In total, 179 and 167 candidate germline mutations were detected in subjects 77 and 92, respectively, but these mutations did not affect known RAS pathway genes or other cancer-related genes, including the ones registered in the pathway databases (Online Methods). A frameshift deletion in *KMT2D* (also known as *MLL2*; encoding p.Val1670fs) was found in subject 92, who had been diagnosed as having Noonan syndrome on the basis of typical features such as hypertelorism, webbed neck and congenital heart disease (Supplementary Fig. 3) but lacked the distinctive facial appearance of Kabuki syndrome, which was shown to be caused by germline *KMT2D* mutations⁵.

Five of the 11 somatic mutations were non-RAS pathway mutations, involving *SETBP1* (3 p.Asp868Asn alterations), *JAK3* (1 p.Arg657Gln alteration) and *SH3BP1* (1 p.Ser277Leu alteration), which had not been reported in JMML cases. *SETBP1* was originally isolated as a 170-kDa nuclear protein that interacts with SET, a small protein inhibitor of the putative tumor suppressors PP2A and NM23-H1 (ref. 6). Several lines of recent evidence suggest that *SETBP1* has a role in leukemogenesis (Supplementary Fig. 4)^{7–11}. *SETBP1* participates in

¹Department of Pediatrics, Nagoya University Graduate School of Medicine, Nagoya, Japan. ²Cancer Genomics Project, Graduate School of Medicine, The University of Tokyo, Tokyo, Japan. ³Laboratory of DNA Information Analysis, Human Genome Center, Institute of Medical Science, The University of Tokyo, Tokyo, Japan. ⁴Department of Pathology and Tumor Biology, Graduate School of Medicine, Kyoto University, Kyoto, Japan. ⁵Laboratory of Sequence Analysis, Human Genome Center, Institute of Medical Science, The University of Tokyo, Tokyo, Japan. ⁶Department of Translational Hematology and Oncology Research, Taussig Cancer Institute, Cleveland Clinic, Cleveland, Ohio, USA. ⁷Department of Hematology and Oncology, Children's Medical Center, Japanese Red Cross Nagoya First Hospital, Nagoya, Japan. ⁸These authors contributed equally to this work. ⁹These authors jointly directed this work. Correspondence should be addressed to S.O. (sogawa-tky@umin.ac.jp) or S.K. (kojimas@med.nagoya-u.ac.jp).

Received 6 November 2012; accepted 17 June 2013; published online 7 July 2013; doi:10.1038/ng.2698



Table 1 List of gene mutations identified by whole-exome sequencing

| Subject number | RAS pathway mutations | | | | | | | | Other somatic mutations | | | |
|-----------------|-----------------------|---------------------|-------------------------|-----------|---------------|---------------------|-------------------------|-----------|-------------------------|---------------------|-------------------------|-----------|
| | Gene | Change at DNA level | Change at protein level | VAFA | Gene | Change at DNA level | Change at protein level | VAFA | Gene | Change at DNA level | Change at protein level | VAFA |
| 11 ^b | <i>NF1</i> | c.4537C>T | p.Arg1513* | 40.1/24.2 | <i>NF1</i> | c.5927delG | p.Trp1976fs | 44.0/47.1 | <i>SETBP1</i> | c.2602G>A | p.Asp868Asn | 32.6/27.0 |
| 63 | <i>KRAS</i> | c.38G>A | p.Gly13Asp | 44.3/0.0 | - | - | - | - | - | - | - | - |
| 72 | <i>PTPN11</i> | c.172A>T | p.Asn58Tyr | 48.2/5.7 | - | - | - | - | <i>SETBP1</i> | c.2602G>A | p.Asp868Asn | 45.9/2.5 |
| | | | | | | | | | <i>JAK3</i> | c.1970G>A | p.Arg657Gln | 30.5/2.2 |
| | | | | | | | | | <i>SH3BP1</i> | c.830C>T | p.Ser277Leu | 47.8/5.1 |
| 77 | - | - | - | - | - | - | - | - | <i>SETBP1</i> | c.2602G>A | p.Asp868Asn | 33.4/2.1 |
| 78 | <i>NRAS</i> | c.35G>C | p.Gly12Ala | 45.5/9.5 | - | - | - | - | - | - | - | - |
| 82 | - | - | - | - | <i>CBL</i> | c.1217del22 | p.Thr406fs | 34.7/38.9 | - | - | - | - |
| 83 | - | - | - | - | <i>NF1</i> | c.4970A>G | p.Tyr1657Cys | 50.0/51.0 | - | - | - | - |
| 84 | - | - | - | - | <i>CBL</i> | c.1096-110del643 | p.Glu366_Phe488del | NA/NA | - | - | - | - |
| 85 | <i>PTPN11</i> | c.226G>A | p.Glu76Lys | 47.5/4.4 | - | - | - | - | - | - | - | - |
| 86 | <i>KRAS</i> | c.38G>A | p.Gly13Asp | 38.9/3.1 | - | - | - | - | - | - | - | - |
| 89 ^c | - | - | - | - | <i>PTPN11</i> | c.1502T>G | p.Ser502Ala | 50.0/49.9 | - | - | - | - |
| 91 ^c | - | - | - | - | <i>PTPN11</i> | c.218C>T | p.Thr73Ile | 49.0/48.0 | - | - | - | - |
| 92 ^c | - | - | - | - | - | - | - | - | - | - | - | - |

NA, not available.

^aVariant allele frequency (VAF) in tumor/reference samples, where the reference was CD3+ T cells, except for subject 63, for whom umbilical cord was used as the reference. ^bSubstantial contamination of tumor cell components in the CD3+ T cell reference. ^cNoonan syndrome-associated myeloproliferative disorder.

translocations that result in an aberrant fusion gene (*NUP98-SETBP1*) and overexpression of *SETBP1* in T cell acute lymphoblastic leukemia (T-ALL) and acute myeloid leukemia (AML), respectively^{12,13}.

SETBP1 is one of the downstream targets induced by the Evi-1 oncoprotein¹⁴ and, together with *EVII* and its homolog *PRDM16* (also known as *MEL1*), was reported to be activated through retrovirus integration.

SETBP1 is also known to augment the recovery of granulopoiesis after gene therapies for chronic granulomatous disease¹⁵. *SETBP1* overexpression is found in more than 27% of adult AML cases and is associated with poor survival¹³. The discovery of recurrent hotspot mutations of *SETBP1* provides unequivocal evidence for the leukemogenic role of deregulated *SETBP1* function. Notably, the *SETBP1* mutation encoding p.Asp868Asn was identical to one of the *de novo* mutations reported to be causative in Schinzel-Giedion syndrome (SGS; MIM 269150), which is a highly recognizable congenital disease characterized by severe mental retardation, distinctive facial features and

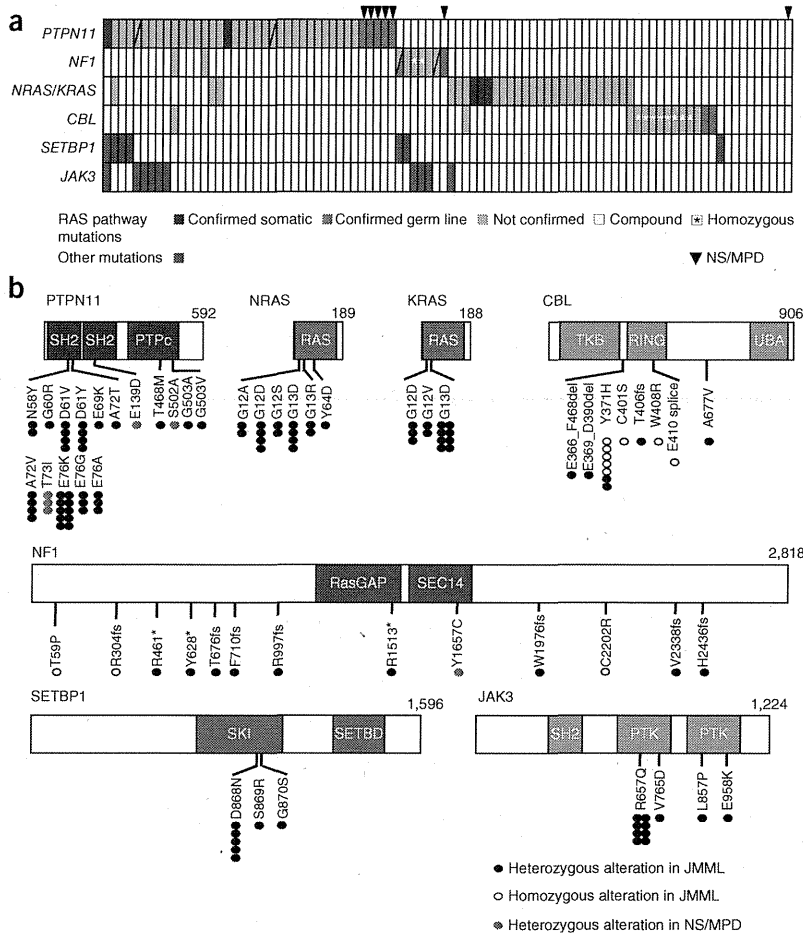


Figure 1 Mutation profiles of 92 JMML cases. (a) The mutation status of RAS pathway genes and 2 newly identified gene targets in a cohort of 92 JMML cases is summarized. NS/MPD, Noonan syndrome-associated myeloproliferative disorder. (b) The distribution of alterations is shown for each protein. SH2, Src homology 2 domain; PTPc, protein tyrosine phosphatase, catalytic domain; RAS, Ras GTPase family domain; TKB, tyrosine kinase-binding domain; RING, RING-finger domain; UBA, ubiquitin-associated domain; RasGAP, a region of similarity with the catalytic domain of the mammalian p120RasGAP protein in neurofibromin; SEC14, Sec14-like lipid-binding domain; SKI, v-ski sarcoma viral oncogene homolog domain; SETBD, SET-binding domain; PTK, pseudokinase domain of the protein tyrosine kinases.

Table 2 Subject characteristics

| Characteristic | Total cohort (n = 92) | Secondary mutations | | P value |
|--|-----------------------|---------------------|----------------|---------|
| | | Yes (n = 16) | No (n = 76) | |
| Sex (male/female) | 61/31 | 12/4 | 49/27 | NS |
| Median age at diagnosis in months (range) | 19 (1–160) | 38 (2–160) | 13 (1–79) | <0.001 |
| Diagnosis | | | | |
| JMML | 85 | 16 | 69 | |
| NS/MPD | 7 | 0 | 7 | |
| Genetic mutations in RAS pathway | | | | |
| <i>PTPN11</i> | 39 | 9 | 30 | NS |
| <i>NF1</i> | 9 | 5 | 4 | 0.001 |
| <i>RAS</i> (<i>NRAS</i> or <i>KRAS</i>) | 28 (15/13) | 2 (1/1) | 26 (14/12) | 0.08 |
| <i>CBL</i> | 14 | 0 | 14 | 0.06 |
| Without RAS pathway mutation | 10 | 1 | 9 | NS |
| Secondary genetic mutations | | | | |
| <i>SETBP1</i> | 7 | 7 | 0 | |
| <i>JAK3</i> | 10 | 10 | 0 | |
| Cytogenetics | | | | |
| Normal karyotype | 77 | 12 | 65 | NS |
| Monosomy 7 | 8 | 1 | 7 | NS |
| Trisomy 8 | 4 | 2 | 2 | NS |
| Other abnormalities | 3 | 1 | 2 | NS |
| WBC count at diagnosis $\times 10^9/l$, median (range) | 30.0 (1.0–563) | 29.6 (5.6–563) | 30.0 (1.0–131) | NS |
| Monocyte count at diagnosis $\times 10^9/l$, median (range) | 4.6 (0.2–31.6) | 3.1 (0.5–15.2) | 4.9 (0.2–31.6) | NS |
| Percent HbF at diagnosis, median (range) | 21 (0–68) | 26 (9–55) | 16 (0–68) | NS |
| PLT at diagnosis $\times 10^9/l$, median (range) | 61.0 (1.4–483) | 47.5 (1.4–175) | 65.0 (5.0–483) | NS |
| HSCT (+/–) | 56/36 | 16/0 | 40/36 | |
| Alive/deceased | 62/30 | 7/9 | 55/21 | |
| Percent probability of 5-year overall survival (95% CI) | 60 (46–71) | 33 (10–59) | 65 (49–77) | 0.10 |
| Percent probability of 5-year transplantation-free survival (95% CI) | 15 (6–27) | 0 (0–0) | 18 (8–33) | 0.007 |

JMML, juvenile myelomonocytic leukemia; NS/MPD, Noonan syndrome-associated myeloproliferative disorder; WBC, white blood cell; HbF, hemoglobin F; HSCT, hematopoietic stem cell transplantation; NS, not significant. We compared the difference between the subjects with and without secondary mutation, and *P* values were calculated by two-sided Fisher's exact test or Mann-Whitney *U* test.

multiple congenital malformations. Individuals with SGS with this mutation have a higher than normal prevalence of tumors, including of neuroepithelial neoplasia¹⁶, although development of myeloid malignancies has not been reported so far.

To further validate our findings, we screened the entire cohort of 92 JMML cases for gene mutations in the newly identified 3 genes

together with known RAS pathway targets using deep sequencing¹⁷ (Supplementary Fig. 5).

RAS pathway mutations were found in 82 of 92 cases (89%) in a mutually exclusive manner, with *PTPN11* mutations predominant, followed by *NRAS*, *KRAS*, *CBL* and *NF1* mutations (Fig. 1a and Table 2). In accordance with previous reports, most of the *CBL* (8/14) and *NF1* (4/9) mutations were biallelic (Fig. 1a,b and Supplementary Table 2)^{2,3,18}, whereas the majority of mutations in *PTPN11*, *NRAS* and *KRAS* were heterozygous⁴. The individuals without RAS pathway mutations (*n* = 10) were vigorously investigated by whole-genome sequencing of tumor-normal paired samples (*n* = 2; Supplementary Fig. 6) or by whole-exome sequencing of only tumor samples (*n* = 8; Supplementary Fig. 7). As anticipated, we found no known RAS pathway mutations.

On the other hand, 18 mutations were found in *SETBP1* (*n* = 7) or *JAK3* (*n* = 11) in 16 cases (Fig. 1a,b, Table 2 and Supplementary Table 2), with these mutations more frequent in cases with mutated *PTPN11* (and possibly *NF1*) than in cases with mutated *NRAS*, *KRAS*

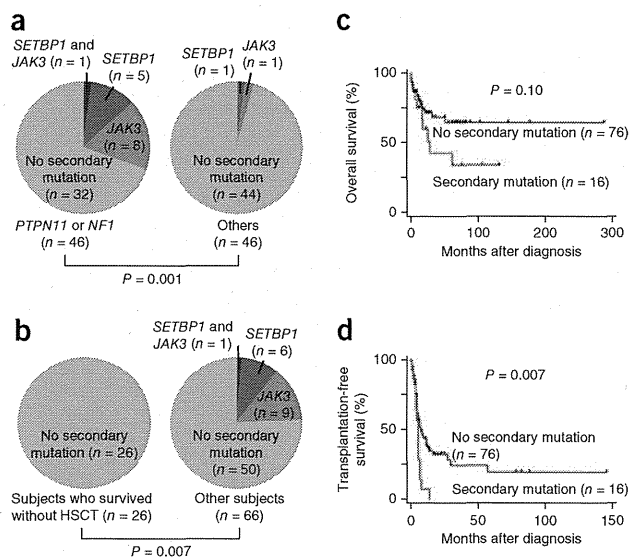


Figure 2 Clinical features of JMML cases with or without secondary mutations. (a,b) Frequency of secondary mutations in individuals with JMML depending on the type of RAS pathway mutations (left, *PTPN11* or *NF1*; right, other or no mutations) (a) and the status of HSCT (b). *P* values were calculated by two-sided Fisher's exact test. (c,d) The impact of secondary mutations on overall (c) and transplantation-free (d) survival is shown in Kaplan-Meier survival curves, where statistical significance was tested by log-rank test.

or *CBL* (Fig. 2a). Mutations in *SH3BP1*, encoding SH3 domain-binding protein 1, were not recurrent. All *SETBP1* mutations were heterozygous and occurred within the portion of the gene encoding the SKI domain, with six identical to the *de novo* recurrent mutations reported in SGS and five identical to the mutation encoding the p.Asp868Asn alteration (Fig. 1b). RT-PCR analysis showed that the wild-type and mutant alleles of *SETBP1* were equally expressed (Supplementary Fig. 8). Similarly, 8 of the 11 *JAK3* mutations in 10 cases were the well-described activating mutation (encoding a p.Arg657Gln alteration) found in various hematological malignancies, including Down syndrome-associated acute megakaryoblastic leukemia^{19–23}, ALL^{24,25} and natural killer (NK)/T cell lymphoma²⁶, and the remaining 3 were also within the portions of the gene encoding the pseudokinase or kinase domain, suggestive of gain of function.

Deep sequencing of the relevant mutant alleles enabled an accurate estimation of allele frequencies for individual mutations (Supplementary Fig. 9). *SETBP1* and *JAK3* mutations showed lower allele frequencies (but not with statistical significance for *SETBP1*) than did the corresponding RAS pathway mutations (Supplementary Fig. 10a), indicating that the former mutations represent secondary genetic hits that contributed to clonal evolution after the main tumor population was established (Supplementary Fig. 10b). Individuals with secondary mutations had shorter lengths of survival compared to those without mutations: 5-year overall survival (hazards ratio (HR) = 1.90, 95% CI = 0.87–4.19). In addition, none of the individuals with JMML who survived without hematopoietic stem cell transplantation (HSCT; *n* = 26) harbored any of the secondary mutations, and individuals with secondary mutations showed significantly inferior 5-year transplant-free survival (HR = 2.18, 95% CI = 1.18–4.02) (Fig. 2b–d and Table 2).

JMML is characterized by a paucity of gene mutations. The average number of mutations per sample (0.85; range of 0–4) was unexpectedly low compared to those reported in other human cancers (Supplementary Fig. 11); excluding common RAS pathway mutations, only 5 mutations were detected in 3 of the 13 discovery cases. This small number of mutations is only comparable to the figure reported for retinoblastoma (mean of 3.3 per case; range of 0–5) (ref. 27) and is in stark contrast to the abundance of gene mutations in chronic myelomonocytic leukemia (CMML) in adult cases, where the mean number of non-silent mutations was 12.4 per sample, of which 3.1 represented known driver changes (ref. 17 and K.Y., M.S., Y.S., D. Nowak, Y. Nagata *et al.*, unpublished data), underscoring the distinct pathogenesis in these two neoplasms that show indistinguishable morphology. The impact of germline events is underscored by the fact that 6 of the 13 discovery cases harbored germline RAS pathway mutations and an additional case without known RAS pathway mutations showed constitutive abnormalities similar to Noonan syndrome. Despite the central role of RAS pathway mutations, a small subset of cases had no documented RAS pathway mutations, even after whole-exome analysis in the two RAS pathway mutation-negative cases, raising the possibility that the latter cases represent a genetically distinct myeloproliferative neoplasm in childhood.

Another key finding in the current study is the discovery of secondary mutations that involve *SETBP1* and *JAK3*. Detected only in a subpopulation of leukemic cells, most of these mutations are thought to be involved in the progression rather than the establishment of JMML and were associated with poor clinical outcome. *SETBP1* is a newly identified proto-oncogene, and identical mutations in this gene have recently been reported in 15–25% of adult cases with atypical chronic myeloid leukemia (CML)¹⁰, CMML and secondary

AML²⁸. Affecting one of three highly conserved amino acid positions, *SETBP1* mutations have been shown to abolish the binding of an E3 ubiquitin ligase (β -TrCP1) to *SETBP1*, which prevents ubiquitination and subsequent degradation, leading to gain of function through the consequent increase in *SETBP1* protein amounts^{10,28}. Although the precise leukemogenic mechanisms of *SETBP1* mutations are still unclear, we have shown that mutant *SETBP1* alleles confer self-renewal capability to myeloid progenitors *in vitro*, and *SETBP1* mutations in adult leukemia were associated with increases in *HOXA9* and *HOXA10* expression²⁸. Recurrent *JAK3* mutations in JMML are also noteworthy. The JAK-STAT pathway is a key component of normal hematopoiesis²⁹. As in other hematopoietic malignancies²⁰, the p.Arg657Gln alteration represents the most frequent change in JMML. This alteration confers interleukin (IL)-3 independence to Ba/F3 cells and induces STAT5 phosphorylation²⁰. Targeting the JAK-STAT pathway with a pan-JAK inhibitor such as CP-690550 (ref. 30) could be a promising therapeutic possibility for patients with *JAK3*-mutated JMML.

In conclusion, our whole-exome sequencing analysis identified the spectrum of gene mutations in JMML. Together with the high frequency of RAS pathway mutations, the paucity of non-RAS pathway mutations is a prominent feature of JMML. Mutations of *SETBP1* and *JAK3* were common recurrent secondary events presumed to be involved in tumor progression and were associated with poor clinical outcomes. Our findings provide an important clue to understanding the pathogenesis of JMML that may help in the development of novel diagnostics and therapeutics for this leukemia.

URLS. Genomon, <http://genomon.hgc.jp/exome/en/>; BioCarta, <http://www.biocarta.com/>; dbSNP131, <http://www.ncbi.nlm.nih.gov/projects/SNP/>; RefSeq database, <http://www.ncbi.nlm.nih.gov/RefSeq/>.

METHODS

Methods and any associated references are available in the online version of the paper.

Accession code. We deposited whole-genome and whole-exome sequence data in the European Genome-phenome Archive under accession EGAS00001000521.

Note: Supplementary information is available in the online version of the paper.

ACKNOWLEDGMENTS

We thank the subjects and their parents for participating in this study. This work was supported by the Research on Measures for Intractable Diseases Project from the Ministry of Health, Labor and Welfare, by Grants-in-Aid from the Ministry of Health, Labor and Welfare of Japan and KAKENHI (23249052, 22134006 and 21790907), by the Project for the Development of Innovative Research on Cancer Therapeutics (P-DIRECT) and by the Japan Society for the Promotion of Science through the Funding Program for World-Leading Innovative R&D on Science and Technology.

AUTHOR CONTRIBUTIONS

H.S., Y.O., H. Muramatsu, K.Y., M.T., A.K. and M.S. designed and performed the research, analyzed the data and wrote the manuscript. Y.S., K.C., H.T. and S.M. performed bioinformatics analyses of the resequencing data. X.W. and Y.X. performed Sanger sequencing. S.D., A.H., K.N., Y.T. and N.Y. collected specimens and performed the research. H. Makishima and J.P.M. designed the research and analyzed the data. S.O. and S.K. led the entire project and wrote the manuscript.

COMPETING FINANCIAL INTERESTS

The authors declare no competing financial interests.

Reprints and permissions information is available online at <http://www.nature.com/reprints/index.html>.

1. Pinkel, D. *et al.* Differentiating juvenile myelomonocytic leukemia from infectious disease. *Blood* **91**, 365–367 (1998).
2. Loh, M.L. *et al.* Mutations in *CBL* occur frequently in juvenile myelomonocytic leukemia. *Blood* **114**, 1859–1863 (2009).
3. Muramatsu, H. *et al.* Mutations of an E3 ubiquitin ligase *c-Cbl* but not *TET2* mutations are pathogenic in juvenile myelomonocytic leukemia. *Blood* **115**, 1969–1975 (2010).
4. Pérez, B. *et al.* Genetic typing of *CBL*, *ASXL1*, *RUNX1*, *TET2* and *JAK2* in juvenile myelomonocytic leukaemia reveals a genetic profile distinct from chronic myelomonocytic leukaemia. *Br. J. Haematol.* **151**, 460–468 (2010).
5. Ng, S.B. *et al.* Exome sequencing identifies *MLL2* mutations as a cause of Kabuki syndrome. *Nat. Genet.* **42**, 790–793 (2010).
6. Minakuchi, M. *et al.* Identification and characterization of SEB, a novel protein that binds to the acute undifferentiated leukemia-associated protein SET. *Eur. J. Biochem.* **268**, 1340–1351 (2001).
7. Damm, F. *et al.* *SETBP1* mutations in 658 patients with myelodysplastic syndromes, chronic myelomonocytic leukemia and secondary acute myeloid leukemias. *Leukemia* **27**, 401–403 (2013).
8. Laborde, R.R. *et al.* *SETBP1* mutations in 415 patients with primary myelofibrosis or chronic myelomonocytic leukemia: independent prognostic impact in CMML. *Leukemia* published online; doi:10.1038/leu.2013.97 (5 April 2013).
9. Meggendorfer, M. *et al.* *SETBP1* mutations occur in 9% of MDS/MPN and in 4% of MPN cases and are strongly associated with atypical CML, monosomy 7, isochromosome i(17)(q10), *ASXL1* and *CBL* mutations. *Leukemia* published online; doi:10.1038/leu.2013.133 (30 April 2013).
10. Piazza, R. *et al.* Recurrent *SETBP1* mutations in atypical chronic myeloid leukemia. *Nat. Genet.* **45**, 18–24 (2013).
11. Thol, F. *et al.* *SETBP1* mutation analysis in 944 patients with MDS and AML. *Leukemia* published online; doi:10.1038/leu.2013.145 (7 May 2013).
12. Panagopoulos, I. *et al.* Fusion of *NUP98* and the SET binding protein 1 (*SETBP1*) gene in a paediatric acute T cell lymphoblastic leukaemia with t(11;18)(p15;q12). *Br. J. Haematol.* **136**, 294–296 (2007).
13. Cristóbal, I. *et al.* *SETBP1* overexpression is a novel leukemogenic mechanism that predicts adverse outcome in elderly patients with acute myeloid leukemia. *Blood* **115**, 615–625 (2010).
14. Goyama, S. *et al.* Evi-1 is a critical regulator for hematopoietic stem cells and transformed leukemic cells. *Cell Stem Cell* **3**, 207–220 (2008).
15. Ott, M.G. *et al.* Correction of X-linked chronic granulomatous disease by gene therapy, augmented by insertional activation of *MDS1-EV11*, *PRDM16* or *SETBP1*. *Nat. Med.* **12**, 401–409 (2006).
16. Hoischen, A. *et al.* De novo mutations of *SETBP1* cause Schinzel-Giedion syndrome. *Nat. Genet.* **42**, 483–485 (2010).
17. Yoshida, K. *et al.* Frequent pathway mutations of splicing machinery in myelodysplasia. *Nature* **478**, 64–69 (2011).
18. Flotho, C. *et al.* Genome-wide single-nucleotide polymorphism analysis in juvenile myelomonocytic leukemia identifies uniparental disomy surrounding the *NFI* locus in cases associated with neurofibromatosis but not in cases with mutant *RAS* or *PTPN11*. *Oncogene* **26**, 5816–5821 (2007).
19. Walters, D.K. *et al.* Activating alleles of *JAK3* in acute megakaryoblastic leukemia. *Cancer Cell* **10**, 65–75 (2006).
20. Sato, T. *et al.* Functional analysis of *JAK3* mutations in transient myeloproliferative disorder and acute megakaryoblastic leukaemia accompanying Down syndrome. *Br. J. Haematol.* **141**, 681–688 (2008).
21. De Vita, S. *et al.* Loss-of-function *JAK3* mutations in TMD and AMKL of Down syndrome. *Br. J. Haematol.* **137**, 337–341 (2007).
22. Norton, A. *et al.* Analysis of *JAK3*, *JAK2*, and *C-MPL* mutations in transient myeloproliferative disorder and myeloid leukemia of Down syndrome blasts in children with Down syndrome. *Blood* **110**, 1077–1079 (2007).
23. Kiyoi, H., Yamaji, S., Kojima, S. & Naoe, T. *JAK3* mutations occur in acute megakaryoblastic leukemia both in Down syndrome children and non-Down syndrome adults. *Leukemia* **21**, 574–576 (2007).
24. Elliott, N.E. *et al.* FERM domain mutations induce gain of function in *JAK3* in adult T-cell leukemia/lymphoma. *Blood* **118**, 3911–3921 (2011).
25. Zhang, J. *et al.* The genetic basis of early T-cell precursor acute lymphoblastic leukaemia. *Nature* **481**, 157–163 (2012).
26. Koo, G.C. *et al.* Janus kinase 3-activating mutations identified in natural killer/T-cell lymphoma. *Cancer Discov.* **2**, 591–597 (2012).
27. Zhang, J. *et al.* A novel retinoblastoma therapy from genomic and epigenetic analyses. *Nature* **481**, 329–334 (2012).
28. Makishima, H. *et al.* Somatic *SETBP1* mutations in myeloid malignancies. *Nat. Genet.* published online; doi:10.1038/ng.2696 (7 July 2013).
29. Crozatier, M. & Meister, M. *Drosophila* haematopoiesis. *Cell. Microbiol.* **9**, 1117–1126 (2007).
30. Changelian, P.S. *et al.* Prevention of organ allograft rejection by a specific Janus kinase 3 inhibitor. *Science* **302**, 875–878 (2003).

ONLINE METHODS

Subjects. We studied 92 children (61 boys and 31 girls) with JMML, including 7 individuals with NS/MPD, who were diagnosed as having JMML in institutions throughout Japan. Written informed consent was obtained from subjects' parents before sample collection. This study was approved by the ethics committees of the Nagoya University Graduate School of Medicine and the University of Tokyo in accordance with the Declaration of Helsinki. Diagnosis with JMML was made on the basis of internationally accepted criteria¹. Characteristics of the 92 JMML cases are summarized in **Table 2**. The median age at diagnosis was 16 months (range of 1–160 months). Karyotypic abnormalities were detected in 16 subjects, including in 8 with monosomy 7. Fifty-six of the 92 subjects (61%) received allogeneic HSCT.

Sample preparation. Genomic DNA was extracted using the QIAamp DNA Blood Mini kit and the QIAamp DNA Investigator kit (Qiagen) according to the manufacturer's instructions. The T Cell Activation/Expansion kit, human (Miltenyi Biotec) was used for the expansion of CD3⁺ T cells from subjects' peripheral blood or bone marrow mononuclear cells³.

Whole-exome sequencing. Exome capture from paired tumor-reference DNA was performed using SureSelect Human All Exon V3 (Agilent Technologies), covering 50 Mb of coding exons, according to the manufacturer's protocol. Enriched exome fragments were subjected to massively parallel sequencing using the HiSeq 2000 platform (Illumina). Candidate somatic mutations were detected through our in-house pipeline (Genomon) as previously described¹⁷.

Detection of mutations from whole-exome sequencing data. Detection of candidate somatic mutations was performed according to previously described algorithms with minor modifications¹⁷. Briefly, the number of reads containing single-nucleotide variations (SNVs) and indels in both tumor and reference samples was determined using SAMtools³¹, and the null hypothesis of equal allele frequencies in tumor and reference samples was tested using the two-tailed Fisher's exact test. A variant was adopted as a candidate somatic mutation if it had $P < 0.01$, if it was observed in bidirectional reads (in both plus and minus strands of the reference sequence) and if its allele frequency was less than 0.25 in the corresponding reference sample. For the detection of germline mutations in RAS pathway genes, SNVs and indels having allele frequencies of more than 0.25 (SNVs) and 0.10 (indels) were interrogated for 46 genes, which consisted of known JMML-related RAS pathway genes and genes registered in the pathway databases ('RAS signaling pathway' in BioCarta and 'signaling to RAS' in Reactome³²). For variant calls in tumor samples for which the paired normal reference was not available, candidate variants in the RAS pathway were detected at an allele frequency of >0.10 . Finally, the list of candidate somatic and/or germline mutations was generated by excluding synonymous SNVs and other variants registered in either dbSNP131 or an in-house SNP database constructed from 180 individual samples. All candidates were validated by Sanger sequencing as previously described.

Estimation of tumor content. The tumor content of bone marrow specimens was estimated from the allele frequency of the somatic mutations identified by deep sequencing. For homozygous mutations, as indicated by an allele frequency of >0.75 , the tumor content (F_{tumor}) was calculated from the observed frequency (F_{observed}) of the mutation according to the following equation: $F_{\text{tumor}} = 2 \times F_{\text{observed}} - 1$. For heterozygous mutations, the tumor content was calculated by doubling the allele frequency.

Power analysis of whole-exome sequencing. The power of detecting somatic mutations at each nucleotide position in whole-exome sequencing was estimated by Monte-Carlo simulation ($n = 1,000$) on the basis of the observed mean depth of coverage for each exon in germline and tumor samples and the observed tumor content for each sample, which were estimated using the allele frequencies of the observed mutations. For the samples with no observed somatic mutations, the average tumor content of the informative samples was employed. Simulations were performed across a total of 192,424 exons.

Copy number analysis in whole-exome sequencing data. To detect copy number lesions at a single-exon level, the mean coverage of each exon

normalized by the mean depth of coverage of the entire sample was compared with that of 12 unrelated normal DNA samples. Exons showing normalized coverage greater than 3 s.d. from the mean coverage of the reference samples were called as candidates for copy number alterations. All candidate exons of RAS pathway genes were visually inspected using the Integrative Genomics Viewer³³ and were validated by Sanger sequencing of corresponding putative breakpoint-containing fragments.

Targeted deep sequencing. Deep sequencing of the targeted genes was performed essentially as described in the 'deep sequencing of pooled target exons' section in ref. 17, except that target DNA was not pooled. Briefly, all exons of *PTPN11*, *NFI*, *KRAS*, *NRAS*, *CBL*, *SETBP1*, *JAK3* and *SH3BP1* were PCR amplified with Quick Taq HS DyeMix (TOYOBO) and the PrimeSTAR GXL DNA Polymerase kit (Takara Bio) using primers including the NotI restriction site (**Supplementary Table 3**). The PCR products from an individual sample were combined and purified with the QIAquick PCR Purification kit (Qiagen) for subsequent digestion with NotI (Fermentas). Digested PCR product was purified, concatenated with T4 DNA ligase (Takara Bio) and sonicated to generate fragments with an average size of 150 bp using Covaris. Fragments were processed for sequencing according to a modified Illumina paired-end library protocol, and sequences were read by a HiSeq 2000 instrument using a 100-bp paired-end read protocol.

Variant calls in targeted deep sequencing. Data processing and variant calling were performed with modifications to the protocol described in a previous publication¹⁷. Each read was aligned to the set of targeted sequences from PCR amplification, with BLAT³⁴ instead of Burrows-Wheeler Aligner (BWA)³⁵ used with the -fine option. Mapping information in the .psl format was converted to the .sam format with paired-read information. Of the successfully mapped reads, reads were excluded from further analysis if they mapped to multiple sites, mapped with more than four mismatched bases or had more than ten soft-clipped bases. Next, the Estimation_CRME script was run to eliminate strand-specific errors and exclude PCR-derived errors. A strand-specific mismatch ratio was calculated for each nucleotide variant for both strands using the bases from read cycles 11 to 50 on the next-generation sequencer. By excluding the top five cycles showing the highest mismatch rates, strand-specific mismatch rates were recalculated, and the smaller value between both strands was adopted as a nominal mismatch ratio for that variant. After excluding variants found in dbSNP131 or the in-house SNP database, non-silent variants having a mismatch ratio of greater than 0.05 were called as candidates, unless they had median values of the mismatch ratio at the relevant nucleotide positions in the 92 samples of greater than 0.01, as such variants were likely to be caused by systematic PCR problems. Finally, candidates with mismatch ratios of >0.15 were further validated by Sanger sequencing.

Annotation of the detected mutations. Detected mutations were annotated using ANNOVAR³⁶. The positions of the mutations were based on the following RefSeq transcript sequences: NM_002834.3 for *PTPN11*, NM_000267.3 for *NFI*, NM_002524.4 for *NRAS*, NM_004985.3 for *KRAS*, NM_005188.3 for *CBL*, NM_015559.2 for *SETBP1* and NM_000215.3 for *JAK3*. The effect of the mutations on protein function was assessed by SIFT³⁷, PolyPhen-2 (ref. 38) and MutationTaster³⁹.

Whole-genome sequencing. Paired tumor-reference DNA samples were sequenced with the HiSeq 2000 platform according to the manufacturer's instructions to obtain 30× read coverage for reference samples and 40× coverage for tumor samples. Obtained FASTQ sequences were aligned to the human reference genome (hg19) using BWA³⁵ 0.5.8 with default parameters. Alignment of pairs of sequences, at least one of which was not mapped or was considered to have possible mapping problems (with mapping quality of less than 40, insertions or deletions, soft-clipped sequence of more than 10% of the length of the original sequence, irregular paired-read orientation or mate distance of greater than 2,000 bp), was attempted with BLAT³⁴ using default parameters, except for stepSize = 5 and repMatch = 2,253. Mapping statistics were calculated by counting the bases at each genomic position with SAMtools³¹. For variant calling, variant and reference bases with base quality of >30 were counted in both germline and tumor samples, and the Fisher's

exact test was applied. Variants with P of <0.01 were called. Variants having allele frequency of >0.25 in the germline sample were excluded. Variants found in 12 unrelated germline samples with an allele frequency of >0.01 on average were also excluded owing to the high probability that they represented false positive calls. Copy number estimation was performed by calculating the averaged ratio of read depths in germline and tumor samples in 10,000-base bins. An allele-specific copy number plot was generated by measuring the allele frequency of the tumor sample at the positions in which more than 25% of the allele mismatch was observed in germline samples. For the detection of chromosomal structural variations, soft-clipped sequences that could be mapped to a unique genomic position were selected. Structural variation candidates that had more than four supporting read pairs in total and at least one read pair from each side of the breakpoint were called. Contig sequences were generated by assembling the reads within 200 bp of the breakpoint with CAP3 (ref. 40), and structural variations having the contig sequence that could be aligned to the alternate assembly of the hg19 genome with more than 93% identity were excluded as false positives. Structural variations with read depth of greater than 150 on at least one side of the breakpoint were considered to be mapped to a repeat element and were also excluded. For detection of viruses, unmapped sequences were aligned to the collection of all viral genomes in the RefSeq database using BLAT. A virus was considered to be detected if its genome was covered by mean read coverage of >1 .

cDNA sequencing. Total RNA was extracted using the RNeasy Mini kit (Qiagen) and was reverse transcribed with the ThermoScript RT-PCR system (Life Technologies). Target sequences were PCR amplified with the PrimeSTAR GXL DNA Polymerase kit using the primers listed in **Supplementary Table 3** and were sequenced.

Statistical analysis. For comparison of the frequency of mutations or other clinical features between disease groups, categorical variables were analyzed using the Fisher's exact test, and continuous variables were tested using the Mann-Whitney U test. Overall survival and transplantation-free survival were estimated by the Kaplan-Meier method. Hazard ratios for survival with 95% CIs were estimated according to the Cox proportional hazards model, and difference in survival was tested by log-rank test. STATA version 12.0 (StataCorp) was used for all statistical calculations.

31. Li, H. *et al.* The Sequence Alignment/Map format and SAMtools. *Bioinformatics* **25**, 2078–2079 (2009).
32. Matthews, L. *et al.* Reactome knowledgebase of human biological pathways and processes. *Nucleic Acids Res.* **37**, D619–D622 (2009).
33. Thorvaldsdóttir, H., Robinson, J.T. & Mesirov, J.P. Integrative Genomics Viewer (IGV): high-performance genomics data visualization and exploration. *Brief. Bioinform.* **14**, 178–192 (2013).
34. Kent, W.J. BLAT—the BLAST-like alignment tool. *Genome Res.* **12**, 656–664 (2002).
35. Li, H. & Durbin, R. Fast and accurate short read alignment with Burrows-Wheeler transform. *Bioinformatics* **25**, 1754–1760 (2009).
36. Wang, K., Li, M. & Hakonarson, H. ANNOVAR: functional annotation of genetic variants from high-throughput sequencing data. *Nucleic Acids Res.* **38**, e164 (2010).
37. Kumar, P., Henikoff, S. & Ng, P.C. Predicting the effects of coding non-synonymous variants on protein function using the SIFT algorithm. *Nat. Protoc.* **4**, 1073–1081 (2009).
38. Adzhubei, I.A. *et al.* A method and server for predicting damaging missense mutations. *Nat. Methods* **7**, 248–249 (2010).
39. Schwarz, J.M., Rödelsperger, C., Schuelke, M. & Seelow, D. MutationTaster evaluates disease-causing potential of sequence alterations. *Nat. Methods* **7**, 575–576 (2010).
40. Huang, X. & Madan, A. CAP3: A DNA sequence assembly program. *Genome Res.* **9**, 868–877 (1999).



Wiskott–Aldrich Syndrome Presenting With a Clinical Picture Mimicking Juvenile Myelomonocytic Leukaemia

Ayami Yoshimi, MD,^{1*} Yoshiro Kamachi, MD,² Kosuke Imai, MD,³ Nobuhiro Watanabe, MD,⁴ Hisaya Nakadate, MD,⁵ Takashi Kanazawa, MD,⁶ Shuichi Ozono, MD,⁷ Ryoji Kobayashi, MD,⁸ Misa Yoshida, MD,⁹ Chie Kobayashi, MD,¹⁰ Asahito Hama, MD,² Hideki Muramatsu, MD,² Yoji Sasahara, MD,¹¹ Marcus Jakob, MD,¹² Tomohiro Morio, MD,¹³ Stephan Ehl, MD,¹⁴ Atsushi Manabe, MD,¹⁵ Charlotte Niemeyer, MD,¹ and Seiji Kojima, MD²

Background. Wiskott–Aldrich syndrome (WAS) is a rare X-linked immunodeficiency caused by defects of the WAS protein (WASP) gene. Patients with WAS typically demonstrate micro-thrombocytopenia. **Procedures.** The report describes seven male infants with WAS that initially presented with leukocytosis, monocytosis, and myeloid and erythroid precursors in the peripheral blood (PB) and dysplasia in the bone marrow (BM), which was initially indistinguishable from juvenile myelomonocytic leukaemia (JMML). **Results.** The median age of affected patients was 1 month (range, 1–4 months). Splenomegaly was absent in four of these patients, which was unusual for JMML. A mutation analysis of genes in the RAS-signalling pathway did not support a diagnosis of JMML. Non-

haematological features, such as eczema (n = 7) and bloody stools (n = 6), ultimately led to the diagnosis of WAS at a median age of 4 months (range, 3–8 months), which was confirmed by absent (n = 6) or reduced (n = 1) WASP expression in lymphocytes by flow cytometry (FCM) and a WASP gene mutation. Interestingly, mean platelet volume (MPV) was normal in three of five patients and six of seven patients demonstrated occasional giant platelets, which was not compatible with WAS. **Conclusions.** These data suggest that WAS should be considered in male infants presenting with JMML-like features if no molecular markers of JMML can be detected. *Pediatr Blood Cancer* 2013;60:836–841.

© 2012 Wiley Periodicals, Inc.

Key words: children; juvenile myelomonocytic leukaemia; Wiskott–Aldrich syndrome

INTRODUCTION

Wiskott–Aldrich syndrome (WAS) is a rare X-linked recessive disorder, characterized by micro-thrombocytopenia, eczematous skin disease, and recurrent infections. The incidence of WAS is 1–10 in 1 million male new-borns. Affected patients have a predisposition to autoimmune diseases and lymphoid malignancies [1,2]. The responsible gene is *WASP*, which encodes the 502 amino acid WASP protein [3]. *WASP* is expressed selectively in hematopoietic cells and is involved in cell signalling and cytoskeleton reorganization [3]. Specific types of defects in *WASP* are often but not invariably associated with the severity of disease and clinical phenotype. Lack of *WASP* expression causes the most severe phenotype (i.e., classic WAS), whereas inactivating *WASP* missense mutations allow residual protein expression and can cause less severe X-linked thrombocytopenia (XLT) [4,5]. Gain-of-function mutations generate X-linked neutropenia (XLN) [6,7].

Juvenile myelomonocytic leukaemia (JMML) is a rare disease in children that occurs with an estimated incidence of 1–2 cases per million [8]. JMML has characteristics of both myelodysplastic syndrome (MDS) and myeloproliferative disorders (MPD) and is categorized in the MDS/MPD category in the World Health Organization (WHO) classification [9–11]. Clinical and haematological manifestations of JMML include hepatosplenomegaly, skin rash, lymphadenopathy, leukoerythroblastosis, monocytosis, and thrombocytopenia. Recent studies show that deregulated activation of the RAS/MAPK signalling pathway plays a central role in the pathogenesis of JMML. Gene mutations in either the *RAS*, *PTPN11*, *NFI*, or *CBL* genes involved in this pathway are detected in about 80% of JMML patients [12–18].

Micro-thrombocytopenia is the key haematological finding in patients with WAS. However, myelopoiesis and erythropoiesis are usually not affected, despite the fact that *WASP* is expressed in various hematopoietic cells [19]. The present report describes seven cases of male infants with classical WAS who demonstrated

haematological abnormalities mimicking JMML. Importantly, patients can present with JMML-like features before the full clinical manifestations of WAS become apparent. Moreover, nor-

¹Department of Paediatrics and Adolescent Medicine, University of Freiburg, Freiburg, Germany; ²Department of Paediatrics, Nagoya University Graduate School of Medicine, Nagoya, Japan; ³Department of Paediatrics, Perinatal and Maternal Medicine, Tokyo Medical and Dental University, Tokyo, Japan; ⁴Division of Haematology and Oncology, Children's Medical Center, Japanese Red Cross Nagoya First Hospital, Nagoya, Japan; ⁵Department of Paediatrics, Kitasato University School of Medicine, Sagami-hara, Japan; ⁶Department of Paediatrics and Developmental Medicine, Gunma University Graduate School of Medicine, Gunma, Japan; ⁷Department of Paediatrics and Child Health, Kurume University School of Medicine, Kurume, Japan; ⁸Department of Paediatrics, Sapporo Hokuyu Hospital, Sapporo, Japan; ⁹Division of Haemato-Oncology/Regeneration Medicine, Kanagawa Children's Medical Center, Kanagawa, Japan; ¹⁰Department of Paediatrics, University of Tsukuba, Tsukuba, Japan; ¹¹Department of Paediatrics, Tohoku University Graduate School of Medicine, Sendai, Japan; ¹²Department of Paediatrics and Adolescent Medicine, University of Regensburg, Regensburg, Germany; ¹³Department of Paediatrics and Developmental Biology, Tokyo Medical and Dental University Graduate School of Medical and Dental Sciences, Tokyo, Japan; ¹⁴Centre of Chronic Immunodeficiency, University of Freiburg, Freiburg, Germany; ¹⁵Department of Paediatrics, St. Luke's International Hospital, Tokyo, Japan

Grant sponsor: Ministry of Health, Labour, and Welfare of Japan, Tokyo.

Conflict of interest: Nothing to report.

*Correspondence to: Ayami Yoshimi, MD, PhD, Department of Paediatrics and Adolescent Medicine, Paediatric Haematology and Oncology, University of Freiburg, Mathildenstrasse 1, 79106 Freiburg, Germany. E-mail: ayami.yoshimi@uniklinik-freiburg.de

Received 22 July 2012; Accepted 11 September 2012

mal mean platelet volume (MPV) and the presence of the giant platelets complicated the diagnostic evaluation in some of our patients.

PATIENTS AND METHODS

Patients

In 2007, we described a case of a male patient (patient #1) with WAS who demonstrated JMML-like clinical features [20]. Briefly, thrombocytopenia was detected shortly after birth. He suffered from bloody diarrhoea from the age of 9 days. At the age of 42 days, leukocytosis with myeloid/erythroid precursors and monocytosis was detected. Bone marrow (BM) aspirates showed hypercellularity with significant predominance of myelopoiesis and dysplastic features. The morphological features were compatible with JMML. Subsequently, the white blood cell (WBC) count increased to $52.0 \times 10^9/L$ with the appearance of peripheral blasts (3%) and persistent fever. Intravenous administration of various antibiotics had no effect on fever and leukocytosis. Oral 6-mercaptopurine (6-MP) was administered, which resulted in disappearance of leukocytosis. Positive results of cytomegalovirus (CMV)-IgM/IgG and a low level pp65 CMV-antigen (Ag) cells were transitionally noted without CMV-related symptoms. Intravenous administration of ganciclovir (GCV) led to the elimination of CMV-Ag but not to any improvement of JMML-like features. At the age of 7 months, mild atopic dermatitis-like eczema was recognized, which finally led to the clinical and molecular diagnosis of WAS.

The MDS committee of the Japanese Society of Paediatric Hematology/Oncology (JSPHO) study coordinating center of the European Working Group of MDS in Childhood (EWOG-MDS) perform the morphological review of peripheral blood (PB) and BM smears and laboratory examinations for the diagnosis of JMML in Japan and Germany, respectively. By January 2011, WAS was diagnosed in six Japanese males (including patient #1) and one German male who were initially referred with a suspected diagnosis of JMML. Patient #4 was recently reported [21]. Approval for the study was obtained from the institutional review board of Nagoya University, Nagoya, Japan, and University of Freiburg, Freiburg, Germany. Informed consent was provided by parents according to the Declaration of Helsinki.

Diagnostic Tests for Wiskott–Aldrich Syndrome

Intracellular WASP expression in lymphocytes was analysed by flow cytometry (FCM) by the standard method described previously [4,22]. DNA purification and sequencing of genomic DNA, RNA isolation, reverse transcription-polymerase chain reaction, and sequencing of cDNA for the mutational analysis of WASP gene was performed as reported previously [23].

Diagnostic Tests for Juvenile Myelomonocytic Leukemia

Mutational screening for *PTPN11*, *NRAS*, and *KRAS* genes was performed in six patients, as previously reported [24–27]. In patients #6 and #7, the *c-CBL* gene, which has been recently found in about 10% of JMML patients, was also screened as described previously [16,18]. None of the patients had clinical signs of neurofibromatosis type 1 (NF1). *In vitro* colony assay for granulocyte–macrophage colony stimulating factor (GM-CSF)

hypersensitivity assay was performed as a supportive diagnostic tool for JMML as previously reported [28,29].

RESULTS

Clinical Characteristics and Laboratory Findings

The clinical characteristics of these patients are summarized in Table I. Thrombocytopenia and bloody diarrhoea were observed soon after birth in all patients except for patient #6. JMML-like clinical manifestations occurred within the first few months of life. Eczema developed between 0 and 3 months after birth in all patients. Splenomegaly was seen in three of seven patients and massive splenomegaly was present in two patients. At the presentation of JMML-like features, episodes of recurrent infections, which suggest an immunodeficiency, were not observed in any patients. However, in three patients, recurrent bacterial, or viral infections (cases #5, #6, and #7) were documented during the clinical course.

The laboratory findings at the presentation of JMML-like disease are summarized in Table II. The WBC count was increased in all patients except for in patient #7. Monocytosis and myeloid/erythroid precursors were seen in PB in all patients. All patients had anaemia. The MPV before platelet transfusions ranged between 6.9 and 7.9 fl (normal, 7.2–11.7 fl) in the five patients that were evaluated. Hb F levels were normal in three patients examined. The platelet morphology demonstrated anisocytosis in all patients. Occasional giant platelets, which are defined as platelets bigger than red cells, were observed in six patients. These features were unusual for WAS. Full BM with significant predominance of myelopoiesis and a marked left shift of the myeloid lineage was seen in all patients. The number of megakaryocytes was normal or increased. Dysplasia in megakaryopoiesis, myelopoiesis, and erythropoiesis was observed in seven, four, and four patients, respectively. The common dysplasia in the megakaryopoiesis included hypolobulations of nuclei and small megakaryocytes with single or double round nuclei. In the myelopoiesis, nuclear abnormalities such as double nuclei, ring nuclei, or pseudo-Pelger-Huet anomaly nuclei were often seen. The dysplasia of erythropoiesis was mild, if observed, and included nuclear lobulation and double nuclei. The karyotype was normal in all patients. The serum levels of immunoglobulin were variable (Table II). Evaluation of T cell function revealed normal responses to phytohemagglutinin and concanavalin A in the four patients that were examined. The numbers of peripheral T and B cells and the CD4/8 ratio were normal in four patients. Patient #7 demonstrated B-lymphocytopenia and an elevated CD4/8 ratio.

Diagnostic Tests for Juvenile Myelomonocytic Leukemia

Molecular analysis of *PTPN11*, *N-RAS*, and *K-RAS* genes ($n = 7$) and the *c-CBL* gene ($n = 2$) documented no mutations in any of the examined patients. *In vitro* GM-CSF hypersensitivity was performed in all patients but patient #1 and was positive only in patient #4.

Diagnostic Tests for Wiskott–Aldrich Syndrome

FCM analysis showed absent ($n = 6$) or reduced ($n = 1$) WASP expression in the lymphocytes, which led to the confirmation of a diagnosis of WAS (Table III). Mutations of WASP genes

TABLE I. Clinical Features of the Patients

| Patient | 1 | 2 | 3 | 4 | 5 | 6 | 7 |
|---|--------------------------|--------------------------|--------------------------|-------------------|-----------------------------|-------------------------|-----------------------------------|
| Age at the detection of thrombocytopenia | At birth | At birth | At birth | At birth | 1 month | 4 months | 2 months |
| Age at the onset of JMML like haematological features | 1 month | 3 months | 1 month | 1 month | 1 month | 4 months | 2 months |
| Age at the onset of eczema | 1 month | 3 months | Soon after birth | 3 months | 1 month | 3 months | 2 months |
| Age at the onset of bloody diarrhoea | At birth | 20 days | At birth | 1 week | 1 month | No | 1 month |
| Hepatomegaly/splenomegaly (cm under the costal margin) | Yes (3)/no | Yes (3)/yes# | No/no | No/no | No/no | Yes (5)/yes (7.5) | Yes (6)/yes (6) |
| Infectious episodes before the diagnosis of WAS | CMV antigenemia | No episode | No episode | No episode | Fever of unknown origin | Otitis media | Adenovirus and Rotavirus in stool |
| Infectious episodes between the diagnosis of WAS and HSCT | No episode | No episode | No episode | No episode | Bacterial and RSV pneumonia | Otitis media | CMV pneumonia |
| | | | | | Rotavirus gastroenteritis | Anal abscess | |
| HSCT (age) | 10 months | 10 months | 17 months | 4 months | 18 months | 13 months | 7 months |
| Donor/stem cell source | U-CBT | MSD-BMT | U-CBT | MSD-BMT | 1 antigen MMUD-BMT | MUD-BMT | MUD-BMT |
| Survival (age at the time of the last follow-up) | Alive (6 years 5 months) | Alive (5 years 4 months) | Alive (4 years 8 months) | Alive (12 months) | Alive (1 year 9 months) | Alive (1 year 6 months) | Alive (1 year 7 months) |

JMML, juvenile myelomonocytic leukaemia; WAS, Wiskott–Aldrich syndrome; RSV, respiratory syncytial virus; CMV, cytomegalovirus; # splenomegaly was noted only by ultrasound; HSCT, hematopoietic stem cell transplantation; U-CBT, unrelated cord blood transplantation; MSD-BMT, bone marrow transplantation from an HLA matched sibling donor; MUD-BMT, BMT from an HLA matched unrelated donor; MMUD-BMT, BMT from an HLA-mismatched unrelated donor.

TABLE II. Laboratory Findings Accompanying the Juvenile Myelomonocytic Leukaemia-Like Haematological Features

| Patient | 1 | 2 | 3 | 4 | 5 | 6 | 7 |
|---------------------------------------|-------------------|-----------|-----------|---------|-----------|-------------------|--------------------------|
| Peripheral blood | | | | | | | |
| WBC count ($\times 10^9/L$) | 35.5–50.0 | 12.0–18.0 | 13.5–22.1 | 15.0 | 35.0–50.0 | 6.0–12.0 | 7.5 |
| Monocyte count ($\times 10^9/L$) | 8.9 | 1.0–1.5 | 8 | 2.3 | 1.1 | 1.0–1.5 | 1.3 |
| Blasts (%) | 3 | 2 | 2 | 4 | 2 | 0 | 1 |
| Immature myeloid/erythroid cells | Yes/Yes | Yes/Yes | Yes/Yes | Yes/Yes | Yes/Yes | Yes/Yes | Yes/Yes |
| Eosinophils (%) | 3 | 12 | 4 | 7 | 2 | 5 | 2 |
| Platelet count ($\times 10^9/L$) | 44 | 40–90 | 31 | 24 | 53 | 11 | 26 |
| MPV (fl) ^a | 7.0 | 7.4 | NE | 6.9 | 7.5 | NE | 7.9 |
| Platelet anisocytosis/giant platelets | Yes/Yes | Yes/Yes | Yes/Yes | Yes/No | Yes/Yes | Yes/Yes | Yes/Yes |
| Hb (g/dl) | 8.9 | 8.0 | 9.2 | 6.1 | 11.6 | 9.5 | 8.0 |
| Bone marrow | | | | | | | |
| Cellularity | Full ^b | Full | Full | Full | Full | Full | Full |
| M/E ratio | 33 | 4 | 7 | 5.4 | 11 | 2 | 2 |
| Blasts (%) | 3.5 | 0.5 | 1 | 0 | 2 | 3.5 | 2 |
| Karyotype | 46,XY | 46,XY | 46,XY | 46,XY | 46,XY | 46,XY | 46,XY |
| Immunological examination | | | | | | | |
| Age at examination (months) | 8 | 5 | 2 | 2 | 10 | 4 | 2/3/5 |
| IgG (mg/dl) | 2,554 | 468 | 638 | 102 | 792 | 3,780 | 1,170/2,120/2,070 |
| IgM (mg/dl) | 156 | 64 | 37 | <5 | 33 | 353 | 122/244/156 |
| IgA (mg/dl) | 49 | 52 | 38 | 39 | 129 | 124 | 25/45.4/58.2 |
| IgE (mg/dl) | 494 | 368 | 89 | 8 | 16 | 1,330 (10 months) | 258/693/7,995 |
| LBT (PHA, ConA) | Normal | Normal | NE | NE | NE | Normal | Normal |
| CD4/8 ratio | Normal | Normal | NE | Normal | NE | Normal | Increased (7.0/22.2/1.1) |

WBC, white blood cell; MPV, mean platelet volume; M/E myeloid-/erythroid-cells; LBT, lymphoblastic test; PHA, phytohemagglutinin; conA, concanavalin A; NE, not evaluated. ^aNormal range (7.2–11.7 fl). ^bThe cellularity was high (full bone marrow), which was normal for infants.

varied between patients. In patient #1, sequencing of WASP cDNA identified five nucleotides (CCGGG) inserted at position c.387 in exon 4, causing a frameshift at codon 140 that gave rise to a premature stop signal at codon 262, as reported previously [20]. Patients #2 and #3 had previously known nonsense mutations in exon 1 and exon 4, which led to the absence of WASP expression and a moderate to severe clinical phenotype of WAS [4,30–32]. Patient #4 had a known deletion in intron 8, which caused a frameshift and absence of WASP expression [4,5]. Patient #5 had a known splice anomaly in intron 6, which reduced expression of WASP and led to a clinical phenotype of either XLP or WAS [4,32]. Patient #6 had known deletion in exon 1, which was associated with a classic WAS phenotype [33]. Patient #7 had a nonsense mutation in exon 1, which has not been previously described.

Clinical Course of Patients

Patient #1 received 6-MP to control leukocytosis. In other patients, the JMML-like features were stable until allogeneic

hematopoietic stem cell transplantation (HSCT), which was performed at the age of 4–18 months. All patients are alive after HSCT at the time of the last follow-up (Table I). Graft failure was observed in patient #7, and a second HSCT is currently planned for this patient.

DISCUSSION

Although WASP is expressed ubiquitously in hematopoietic cells and although *in vitro* results suggest that WASP is involved in the proliferation and differentiation of all hematopoietic progenitors, overt defects are restricted to micro-thrombocytopenia and immune-dysfunction in classical WAS. We previously described a case of a male presenting with a clinical picture of JMML, in whom WAS was ultimately diagnosed (patient #1) [20]. These haematological abnormalities had not been previously reported in patients with WAS. Since then, we have encountered six additional patients with WAS who presented with similar clinical characteristics. Morphological features were not distinguishable from JMML. Moreover, normal MPV and the presence

TABLE III. Results of the Diagnostic Tests for Wiskott–Aldrich Syndrome

| Patient | 1 | 2 | 3 | 4 | 5 | 6 | 7 |
|--------------------------|------------------------|----------|----------|---------------------------------|------------------------|-----------------------|----------|
| Age at examinations | 8 months | 4 months | 4 months | 3 months | 8 months | 4 months | 3 months |
| WASP protein expression | Absence | Absence | Absence | Absence | Reduced | Absence | Absence |
| WASP mutation | Exon 4 | Exon 1 | Exon 4 | Intron 8 | Intron 6 | Exon 1 | Exon 1 |
| | c.387–421 ins 5nt | c.37C>T | c.424C>T | c.777+1 ₋ +4 delGTGA | c.559+5G>A | c.31delG | c.C55>T |
| Mutation type | Insertion | Nonsense | Nonsense | Deletion | Splice anomaly | Deletion | Nonsense |
| Predicted protein change | Frameshift stop aa 262 | R13X | Q142X | Frameshift stop aa 246 | Frameshift stop aa 190 | Frameshift stop aa 37 | Q19X |

of giant platelets in three and six patients, respectively, initially argued against a diagnosis of WAS, because micro-thrombocytes are known as a key diagnostic feature of WAS and XLP. The JMML-like features developed shortly after birth in all patients, before the full clinical picture of WAS become apparent. In our patients with JMML-like features, signs of immune defects were not present. Without recent advances in molecular diagnostic tests for WAS and JMML, it might otherwise be impossible to establish a diagnosis of WAS in these patients. Absent or reduced WASP expression by FCM-WASP and detection of WASP mutation ultimately led to a diagnosis of WAS. The mutations were distributed in different exons and introns, and there was no clustering. Thrombocytopenia since birth and some of the observed clinical features (e.g., atopic dermatitis-like eczema, persistent bloody stool, lack of splenomegaly) were unusual for JMML but were compatible with WAS.

The deregulated RAS signalling pathway plays a central role in the pathogenesis of JMML, and mutational analyses of *PTPN11*, *RAS*, and *c-CBL* genes located in the RAS signalling pathway have become important diagnostic tests. Mutations of one of these genes and a clinical diagnosis of NF1 can be found in more than 80% of patients with JMML. However, in up to 20% of patients without any molecular markers, a diagnosis of JMML relies on unspecific clinical and laboratory observations. We suggest that WAS should be considered within the differential diagnosis in male infants with clinical features of JMML if no mutations of the RAS signalling pathway can be detected. Importantly, clinicians should not exclude a diagnosis of WAS if the MPV is normal or if giant platelets are present. Rarely, patients with WAS can present with normal or large platelets [34,35].

The pathogenesis of JMML-like feature in these patients is unknown. There is no evidence that WASP is related to the RAS signalling pathway. The activation of this pathway does not seem to be a major cause of JMML-like features in our patients, because GM-CSF hypersensitivity was demonstrated only in one of six patients examined. Patients with WAS have an increased risk of viral infections. CMV, Epstein-Barr virus (EBV) and human herpes virus-6 (HHV-6) infections can mimic JMML in infants [36,37]. However, extensive screening failed to detect viral infections at the time, at which these patients presented with JMML-like features, except for patient #1, in whom CMV antigen was detected.

Leukocyte adhesion deficiency (LAD)-1 is a rare immunodeficiency caused by a mutation in the beta-2 integrin gene. The firm adhesion of leukocyte to the blood vessel wall is defective in LAD-1, which results in leukocytosis, mimicking JMML [38]. A defect of leukocyte adhesion due to abnormal integrin beta clustering has been described in the context of WAS [39]. A mechanism similar to that seen in LAD1 may be present in WAS with JMML-like features.

A recent report showed that WASP localizes to not only the cytoplasm but also to the nucleus and has a role in the transcriptional regulation at the chromatin level in lymphocytes [40]. Active WASP mutations, which cluster within the GTP-ase binding domain of WASP (L270P, S272P, and I294T), cause XLN and myelodysplasia [6,7]. Further, increased apoptosis associated with increased genomic instability in myeloid cells and lymphocytes has been described in the context of active WASP mutations [41,42]. Further research may identify new roles of WASP in transcriptional regulation and genomic stability in haematopoiesis, which may explain the JMML-like features, seen in WAS patients.

In conclusion, WAS should be considered in the differential diagnosis in male infants presenting with JMML-like features if no molecular markers of JMML can be demonstrated. A normal MPV and the presence of giant platelets do not exclude a diagnosis of WAS. Clinical information, such as bloody stool and eczema, may be helpful in pursuing a diagnosis of WAS in an infant with JMML like features.

ACKNOWLEDGMENT

We thank the members of the MDS committee of the JSPHO and the EWOG-MDS. We also thank Dr. Masahumi Onodera (National Medical Center for Children and Mothers Research Institute, Tokyo, Japan) and Dr. Klaus Schwarz (Institute for Transfusion Medicine, University of Ulm, Ulm, Germany) for the mutational analysis of the WASP gene in patients #5 and #7, respectively. We also thank Dr. Eva Jacobsen and Dr. Ansgar Schulz (Department of Paediatrics and Adolescent Medicine, University Hospital Ulm, Ulm, Germany) for FACS analysis of WASP expression in patient #7 and thank Dr. Kenichi Koike (Shinshu University School of Medicine, Matsumoto, Japan), Dr. Christian Flotho and Dr. Thomas Gorr for the mutational analysis of *PTPN11*, *RAS*, *c-CBL* gens in patients #6 and #7.

REFERENCES

- Bosticardo M, Marangoni F, Aiuti A, et al. Recent advances in understanding the pathophysiology of Wiskott-Aldrich syndrome. *Blood* 2009;113:6288-6295.
- Thrasher AJ, Burns SO. WASP: A key immunological multitasker. *Nat Rev Immunol* 2010;10:182-192.
- Derry JM, Ochs HD, Francke U. Isolation of a novel gene mutated in Wiskott-Aldrich syndrome. *Cell* 1994;78:635-644.
- Imai K, Morio T, Zhu Y, et al. Clinical course of patients with WASP gene mutations. *Blood* 2004;103:456-464.
- Jin Y, Mazza C, Christie JR, et al. Mutations of the Wiskott-Aldrich syndrome protein (WASP): Hotspots, effect on transcription, and translation and phenotype/genotype correlation. *Blood* 2004;104:4010-4019.
- Devriendt K, Kim AS, Mathijs G, et al. Constitutively activating mutation in WASP causes X-linked severe congenital neutropenia. *Nat Genet* 2001;27:313-317.
- Ancliff PJ, Blundell MP, Cory GO, et al. Two novel activating mutations in the Wiskott-Aldrich syndrome protein result in congenital neutropenia. *Blood* 2006;108:2182-2189.
- Hasle H, Wadsworth LD, Massing BG, et al. A population-based study of childhood myelodysplastic syndrome in British Columbia, Canada. *Br J Haematol* 1999;106:1027-1032.
- Baumann I, Benett J, Niemeyer CM, et al. Juvenile myelomonocytic leukemia. In: Swerdlow S, Campo E, Harris N, et al, editors. WHO classification of tumors of haematopoietic and lymphoid tissues. Lyon: IARC Press; 2008. 82-86.
- Niemeyer CM, Arico M, Basso G, et al. Chronic myelomonocytic leukemia in childhood: A retrospective analysis of 110 cases. European Working Group on Myelodysplastic Syndromes in Childhood (EWOG-MDS). *Blood* 1997;89:3534-3543.
- Yoshimi A, Kojima S, Hirano N. Juvenile myelomonocytic leukemia: Epidemiology, etiopathogenesis, diagnosis, and management considerations. *Paediatr Drugs* 2010;12:11-21.
- Tartaglia M, Niemeyer CM, Song X, et al. Somatic *PTPN11* mutations in juvenile myelomonocytic leukemia, myelodysplastic syndromes and acute myeloid leukemia. *Nat Genet* 2003;34:148-150.
- Flotho C, Valecannon S, Mach-Pascuala S, et al. RAS mutations and clonality analysis in children with juvenile myelomonocytic leukemia (JMML). *Leukemia* 1999;13:32-37.
- Side L, Taylor B, Cayouette M, et al. Homozygous inactivation of the NF1 gene in bone marrow cells from children with neurofibromatosis type 1 and malignant myeloid disorders. *N Engl J Med* 1997;336:1713-1720.
- Le DT, Kong N, Zhu Y, et al. Somatic inactivation of *Nf1* in hematopoietic cells results in a progressive myeloproliferative disorder. *Blood* 2004;103:4243-4250.
- Niemeyer CM, Kang MW, Shin DH, et al. Germline CBL mutations cause developmental abnormalities and predispose to juvenile myelomonocytic leukemia. *Nat Genet* 2010;42:794-800.
- Loh ML, Sakai DS, Flotho C, et al. Mutations in CBL occur frequently in juvenile myelomonocytic leukemia. *Blood* 2009;114:1859-1863.
- Muramatsu H, Makishima H, Jankowska AM, et al. Mutations of an E3 ubiquitin ligase c-Cbl but not TET2 mutations are pathogenic in juvenile myelomonocytic leukemia. *Blood* 2010;115:1969-1975.
- Kajiwaru M, Nonoyama S, Eguchi M, et al. WASP is involved in proliferation and differentiation of human haemopoietic progenitors in vitro. *Br J Haematol* 1999;107:254-262.
- Watanabe N, Yoshimi A, Kamachi Y, et al. Wiskott-Aldrich syndrome is an important differential diagnosis in male infants with juvenile myelomonocytic leukemia-like features. *J Pediatr Hematol Oncol* 2007;29:836-838.
- Sano H, Kobayashi R, Suzuki D, et al. Wiskott-Aldrich syndrome with unusual clinical features similar to juvenile myelomonocytic leukemia. *Int J Hematol* 2012;96:279-283.
- Yamada M, Ariga T, Kawamura N, et al. Determination of carrier status for the Wiskott-Aldrich syndrome by flow cytometric analysis of Wiskott-Aldrich syndrome protein expression in peripheral blood mononuclear cells. *J Immunol* 2000;165:1119-1122.
- Itoh S, Nonoyama S, Morio T, et al. Mutations of the WASP gene in 10 Japanese patients with Wiskott-Aldrich syndrome and X-linked thrombocytopenia. *Int J Hematol* 2000;71:79-83.

24. Yoshida N, Yagasaki H, Xu Y, et al. Correlation of clinical features with the mutational status of GM-CSF signaling pathway-related genes in juvenile myelomonocytic leukemia. *Pediatr Res* 2009;65:334-340.
25. Yamamoto T, Isomura M, Xu Y, et al. PTPN11, RAS and FLT3 mutations in childhood acute lymphoblastic leukemia. *Leuk Res* 2006;30:1085-1089.
26. Mitani K, Hangaishi A, Imamura N, et al. No concomitant occurrence of the N-ras and p53 gene mutations in myelodysplastic syndromes. *Leukemia* 1997;11:863-865.
27. Tartaglia M, Martinelli S, Cazzaniga G, et al. Genetic evidence for lineage-related and differentiation stage-related contribution of somatic PTPN11 mutations to leukemogenesis in childhood acute leukemia. *Blood* 2004;104:307-313.
28. Emanuel PD, Bates LJ, Castleberry RP, et al. Selective hypersensitivity to granulocyte-macrophage colony-stimulating factor by juvenile chronic myeloid leukemia hematopoietic progenitors. *Blood* 1991;77:925-929.
29. Emanuel PD, Bates LJ, Zhu SW, et al. The role of monocyte-derived hemopoietic growth factors in the regulation of myeloproliferation in juvenile chronic myelogenous leukemia. *Exp Hematol* 1991;19:1017-1024.
30. Jo EK, Futatani T, Kanegane H, et al. Mutational analysis of the WASP gene in 2 Korean families with Wiskott-Aldrich syndrome. *Int J Hematol* 2003;78:40-44.
31. Qasim W, Gilmour KC, Heath S, et al. Protein assays for diagnosis of Wiskott-Aldrich syndrome and X-linked thrombocytopenia. *Br J Haematol* 2001;113:861-865.
32. Lemahieu V, Gastier JM, Francke U. Novel mutations in the Wiskott-Aldrich syndrome protein gene and their effects on transcriptional, translational, and clinical phenotypes. *Hum Mutat* 1999;14:54-66.
33. Ariga T, Yamada M, Sakiyama Y. Mutation analysis of five Japanese families with Wiskott-Aldrich syndrome and determination of the family members' carrier status using three different methods. *Pediatr Res* 1997;41:535-540.
34. Patel PD, Samanich JM, Mitchell WB, et al. A unique presentation of Wiskott-Aldrich syndrome in relation to platelet size. *Pediatr Blood Cancer* 2011;56:1127-1129.
35. Knox-Macaulay HH, Bashawri L, Davies KE. X linked recessive thrombocytopenia. *J Med Genet* 1993;30:968-969.
36. Manabe A, Yoshimasu T, Ebihara Y, et al. Viral infections in juvenile myelomonocytic leukemia: Prevalence and clinical implications. *J Pediatr Hematol Oncol* 2004;26:636-641.
37. Herrod HG, Dow LW, Sullivan JL. Persistent Epstein-Barr virus infection mimicking juvenile chronic myelogenous leukemia: Immunologic and hematologic studies. *Blood* 1983;61:1098-1104.
38. Karow A, Baumann I, Niemeyer CM. Morphologic differential diagnosis of juvenile myelomonocytic leukemia-pitfalls apart from viral infection. *J Pediatr Hematol Oncol* 2009;31:380.
39. Zhang H, Schaff UY, Green CE, et al. Impaired integrin-dependent function in Wiskott-Aldrich syndrome protein-deficient murine and human neutrophils. *Immunity* 2006;25:285-295.
40. Taylor MD, Sadhukhan S, Kottangada P, et al. Nuclear role of WASP in the pathogenesis of dysregulated TH1 immunity in human Wiskott-Aldrich syndrome. *Sci Transl Med* 2010;2:37ra44.
41. Westerberg LS, Meelu P, Baptista M, et al. Activating WASP mutations associated with X-linked neutropenia result in enhanced actin polymerization, altered cytoskeletal responses, and genomic instability in lymphocytes. *J Exp Med* 2010;207:1145-1152.
42. Moulding DA, Blundell MP, Spiller DG, et al. Unregulated actin polymerization by WASP causes defects of mitosis and cytokinesis in X-linked neutropenia. *J Exp Med* 2007;204:2213-2224.

- 2 Martineau AR, Newton SM, Wilkinson KA, *et al.* Neutrophil-mediated innate immune resistance to mycobacteria. *J Clin Invest* 2007; 117: 1988–1994.
- 3 Sugawara I, Udagawa T, Yamada H. Rat neutrophils prevent the development of tuberculosis. *Infect Immun* 2004; 72: 1804–1806.
- 4 Nandi B, Behar SM. Regulation of neutrophils by interferon- γ limits lung inflammation during tuberculosis infection. *J Exp Med* 2011; 208: 2251–2262.
- 5 Brahmabhatt S, Black GF, Carroll NM, *et al.* Immune markers measured before treatment predict outcome of intensive phase tuberculosis therapy. *Clin Exp Immunol* 2006; 146: 243–252.
- 6 Martineau AR, Timms PM, Bothamley GH, *et al.* High-dose vitamin D₃ during intensive-phase antimicrobial treatment of pulmonary tuberculosis: a double-blind randomised controlled trial. *Lancet* 2011; 377: 242–250.
- 7 Lawn SD, Kerkhoff AD, Vogt M, *et al.* Characteristics and early outcomes of patients with Xpert MTB/RIF-negative pulmonary tuberculosis diagnosed during screening before antiretroviral therapy. *Clin Infect Dis* 2012; 54: 1071–1079.
- 8 Lefebvre N, Falzon D. Risk factors for death among tuberculosis cases: analysis of European surveillance data. *Eur Respir J* 2008; 31: 1256–1260.
- 9 Sloand E. Hematologic complications of HIV infection. *AIDS Rev* 2005; 7: 187–196.
- 10 Ferrand RA, Herman J, Elgalib A, *et al.* Septic shock and multi-organ failure in HIV infection – ‘sepsis tuberculosa gravissima’. *Int J STD AIDS* 2006; 17: 562–564.

Eur Respir J 2013; 42: 1752–1757 | DOI: 10.1183/09031936.00140913 | Copyright ©ERS 2013

Pulmonary fibrosis in dyskeratosis congenita with *TINF2* gene mutation

To the Editor:

Dyskeratosis congenita is a rare inherited disorder of ectodermal dysplasia characterised by the classical mucocutaneous triad of abnormal skin pigmentation, nail dystrophy and leukoplakia [1–3], at least one of which is present in around 80–90% of dyskeratosis congenita cases. Bone marrow failure is another common feature, and a variety of other abnormalities (*e.g.* dental, gastrointestinal, neurological, ophthalmic, pulmonary and skeletal) have been also described [1–3]. The main causes of mortality in dyskeratosis congenita are bone marrow failure, pulmonary disease and malignancy [1]. Three modes of inheritance have been recognised: X-linked recessive, autosomal dominant and autosomal recessive [1, 3]. Eight dyskeratosis congenita genes (*DKC1* (dyskeratosis congenita 1), *TERC* (telomerase RNA component), *TERT* (telomerase reverse transcriptase), *NOP10* (nucleolar protein 10), *NHP2*, *TINF2* (TERF1-interacting nuclear factor 2), *TCAB1* and *RTEL1* (regulation of telomere elongation helicase 1)) have already been identified, and their mutations account for ~60% of all dyskeratosis congenita cases [1]. Among the dyskeratosis congenita genes, mutations in *TERC*, *TERT* and *DKC1* have recently been reported to be associated with familial pulmonary fibrosis and idiopathic pulmonary fibrosis, and pulmonary fibrosis is recognised as one of the features of dyskeratosis congenita. However, the relationship between mutations in the other dyskeratosis congenita genes and pulmonary fibrosis has not yet been clarified. To the best of our knowledge, this is the first case report describing a dyskeratosis congenita patient with pulmonary fibrosis who had a *TINF2* mutation.

A 43-year-old female visited our hospital with cough and progressive dyspnoea. She had never smoked, and had a history of aplastic anaemia, ocular pemphigoid, erythroplasia of Queyrat and infertility. Her father had been diagnosed as having aplastic anaemia and his whole body was pigmented. About 2 years ago, she complained of cough and consulted her personal doctor. Her chest radiographs showed diffuse reticular shadows in the bilateral lung fields. She was referred to a general hospital and was diagnosed with idiopathic interstitial pneumonia. Because her general condition was stable at that time, she was followed up without any specific therapy for 1 year. She was referred to our hospital due to gradual worsening of dyspnoea and admitted for further examinations. Her physical examination was remarkable for skin pigmentation on her whole body, ocular pemphigoid in the left eye and fine crackles in both lung fields. Her fingertip skin was rough but her nails were not dystrophic. Although no leukoplakia was found in the oral mucosa, she had erythroplasia of Queyrat of the vulva. Laboratory data showed elevated lactate dehydrogenase, transaminases, erythrocyte sedimentation rate and sialylated carbohydrate antigen KL-6 with thrombocytopenia. Chest radiographs demonstrated consolidation and reticular shadows in the bilateral lung fields. Furthermore, chest computed tomography revealed consolidation and reticular shadows in both lung fields, as well as bronchiectasis and cystic shadows in the left lung.

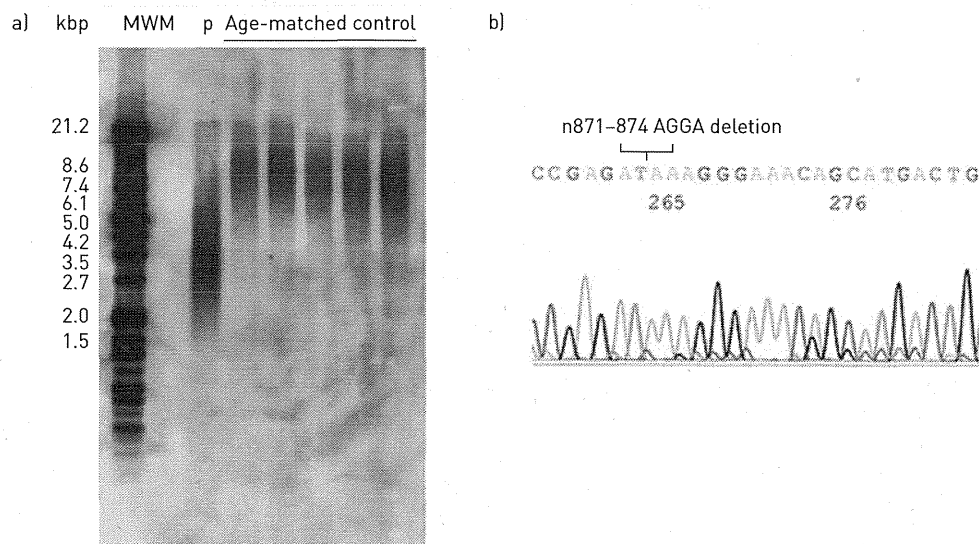


FIGURE 1 a) Southern blot analysis showed shorter telomere length of the patient (P) compared to age-matched healthy controls. MWM: molecular weight marker. b) Gene mutation analysis by direct sequencing showed n871–874 tetranucleotide AGGA deletion in *TINF2* gene.

At this point, we strongly suspected that she had dyskeratosis congenita. To make a definite diagnosis, we first examined the *TERC* and *TERT* genes by direct sequencing. However, no mutations were found in either gene. Southern blot analysis showed short telomere length (fig. 1a), therefore mutations in *TINF2* were next explored. As shown in figure 1b, because direct sequencing showed a n871–874 tetranucleotide AGGA deletion in *TINF2*, she was diagnosed as having dyskeratosis congenita with pulmonary fibrosis associated with *TINF2* mutation. As her respiratory condition progressed, steroid pulse therapy followed by oral prednisolone was conducted. However, no improvement of her symptoms was observed, and bilateral pneumothorax with mediastinal and subcutaneous emphysemas developed. She died of respiratory failure 1 year after starting the treatment.

Dyskeratosis congenita is a rare genetic ectodermal disorder characterised by skin hyperpigmentation, nail dystrophy and leukoplakia of the mucous membranes. Bone marrow failure is a frequent finding and a predisposition to malignancy has been noted. Although pulmonary manifestations of dyskeratosis congenita were believed to be uncommon, DOKAL [1] reported that abnormal pulmonary features may be seen in as many as 10–15% of patients.

Genetically, dyskeratosis congenita is heterogeneous, with three forms having been identified: X-linked recessive, autosomal dominant and autosomal recessive. In the present case, the patient's father had suffered from the same disease; therefore, we suspected that the form of dyskeratosis of this patient was autosomal dominant. The autosomal dominant form of dyskeratosis congenita is caused by heterozygous mutations in the core components of telomerase, *TERC* [4, 5] and *TERT* [6, 7], as well as in the component of the shelterin telomere protection complex, *TINF2* [3]. In this patient, mutation of *TINF2*, but not *TERC* and *TERT*, was confirmed by gene mutation analysis. It has previously been reported that mutations in *DKC1* [8], *TERC* [5] and *TERT* [6] were associated with pulmonary fibrosis in dyskeratosis congenita patients. *DKC1* was not analysed in this patient, because mutation in *DKC1* causes the X-linked form of dyskeratosis congenita. Regarding the relationship between pulmonary fibrosis and *TINF2* mutation in dyskeratosis congenita, WALNE *et al.* [3] have reported that only one patient had pulmonary fibrosis among other clinical features in 33 dyskeratosis congenita patients with *TINF2* mutations. However, they did not describe the patient in detail. To the best of our knowledge, this is the first case report showing pulmonary fibrosis in dyskeratosis congenita with *TINF2* mutation.

TINF2 mutations were reported to be heterozygous mutations in the sixth-found dyskeratosis congenita gene by SAVAGE *et al.* [9] in 2008. *TINF2* encodes TIN2, and is a component of the shelterin telomere-protection complex. The shelterin complex has at least three effects on telomeres: it determines the structure of the telomeric terminus, is implicated in the generation of t-loops and controls the synthesis of telomeric DNA by telomerase [1, 10]. Without the protective activity of shelterin, telomeres are no longer hidden from DNA repair mechanisms and chromosome ends are therefore incorrectly processed by the DNA repair pathways. Approximately 11% of all dyskeratosis congenita has been reported to be accounted for by *TINF2*

mutations and patients with these mutations have significantly shorter telomeres than those with other dyskeratosis congenita subtypes [3]. It has also been reported that most patients with dyskeratosis congenita with *TINF2* mutations have severe disease, and, compared with other dyskeratosis congenita genes, patients with *TINF2* mutations have a high incidence of aplastic anaemia before the age of 10 years [3].

Aberrant repair process by enhanced apoptosis of alveolar epithelial cells plays a critical role in the pathogenesis of pulmonary fibrosis such as idiopathic pulmonary fibrosis, although the precise mechanism is still unclear. The mechanism(s) of pulmonary fibrosis in dyskeratosis congenita has also not yet been clarified. However, because mutations in dyskeratosis congenita genes cause short telomere length with functional deficits in telomere maintenance, telomeres in alveolar epithelial cells may be short. In patients with dyskeratosis congenita, we speculate that aberrant lung repair by enhanced cell death causes pulmonary fibrosis, although the short telomere length in alveolar epithelial cells has not been directly demonstrated.

Herein, we describe the first case report of dyskeratosis congenita with pulmonary fibrosis associated with *TINF2* mutation. This report proved that mutations not only in *TERC*, *TERT* and *DKC1*, but also *TINF2*, cause pulmonary fibrosis in dyskeratosis congenita. However, we do not know why mutations in *TERC*, *TERT* and *DKC1* are frequently found in dyskeratosis congenita patients with pulmonary fibrosis in contrast to the other five genes. In addition, sex hormones, which can increase telomerase activity, are potential therapeutic drugs; however, no standard treatment has been established for pulmonary fibrosis in dyskeratosis congenita patients. Because the clinical characteristics and pathogenesis of pulmonary fibrosis in dyskeratosis congenita is not clear, the accumulation of case-based reports sheds light on the understanding of this devastating disease.



@ERSpublications

The first reported case of a dyskeratosis congenita patient with pulmonary fibrosis and *TINF2* mutation <http://ow.ly/pheRW>

Atsuro Fukuhara¹, Yoshinori Tanino¹, Taeko Ishii¹, Yayoi Inokoshi¹, Kazue Saito¹, Naoko Fukuhara¹, Suguru Sato¹, Junpei Saito¹, Takashi Ishida¹, Hiroki Yamaguchi² and Mitsuru Munakata¹

¹Dept of Pulmonary Medicine, Fukushima Medical University School of Medicine, Fukushima, and ²Division of Hematology, Dept of Internal Medicine, Nippon Medical School, Tokyo, Japan.

Correspondence: Y. Tanino, Dept of Pulmonary Medicine, Fukushima Medical University, 1 Hikarigaoka, Fukushima-City, Fukushima 960-8157, Japan. E-mail: ytanino@fmu.ac.jp

Received: Aug 27 2013 | Accepted after revision: Sept 04 2013 | First published online: Sept 26 2013

Conflict of interest: None declared.

References

- 1 Dokal I. Dyskeratosis congenita. *Hematology Am Soc Hematol Educ Program* 2011; 2011: 480–486.
- 2 Vulliamy TJ, Marrone A, Knight SW, *et al*. Mutations in dyskeratosis congenita: their impact on telomere length and the diversity of clinical presentation. *Blood* 2006; 107: 2680–2685.
- 3 Walne AJ, Vulliamy T, Beswick R, *et al*. *TINF2* mutations result in very short telomeres: analysis of a large cohort of patients with dyskeratosis congenita and related bone marrow failure syndromes. *Blood* 2008; 112: 3594–3600.
- 4 Vulliamy T, Marrone A, Goldman F, *et al*. The RNA component of telomerase is mutated in autosomal dominant dyskeratosis congenita. *Nature* 2001; 413: 432–435.
- 5 Marrone A, Sokhal P, Walne A, *et al*. Functional characterization of novel telomerase RNA (*TERC*) mutations in patients with diverse clinical and pathological presentations. *Haematologica* 2007; 92: 1013–1020.
- 6 Armanios M, Chen JL, Chang YP, *et al*. Haploinsufficiency of telomerase reverse transcriptase leads to anticipation in autosomal dominant dyskeratosis congenita. *Proc Natl Acad Sci USA* 2005; 102: 15960–15964.
- 7 Yamaguchi H, Calado RT, Ly H, *et al*. Mutations in *TERT*, the gene for telomerase reverse transcriptase, in aplastic anemia. *N Engl J Med* 2005; 352: 1413–1424.
- 8 Safa WF, Lestringant GG, Frossard PM. X-linked dyskeratosis congenita: restrictive pulmonary disease and a novel mutation. *Thorax* 2001; 56: 891–894.
- 9 Savage SA, Giri N, Baerlocher GM, *et al*. *TINF2*, a component of the shelterin telomere protection complex, is mutated in dyskeratosis congenita. *Am J Hum Genet* 2008; 82: 501–509.
- 10 de Lange T. Shelterin: the protein complex that shapes and safeguards human telomeres. *Genes Dev* 2005; 19: 2100–2110.

Eur Respir J 2013; 42: 1757–1759 | DOI: 10.1183/09031936.00149113 | Copyright ©ERS 2013

Two cases of partial dominant interferon- γ receptor 1 deficiency that presented with different clinical courses of bacille Calmette–Guérin multiple osteomyelitis

Kaoru Obinata · Tsubasa Lee · Takahiro Niizuma ·
Keiji Kinoshita · Toshiaki Shimizu ·
Takayuki Hoshina · Yuka Sasaki · Toshiro Hara

Received: 2 May 2012 / Accepted: 21 September 2012 / Published online: 11 October 2012
© Japanese Society of Chemotherapy and The Japanese Association for Infectious Diseases 2012

Abstract We experienced two cases of unrelated Japanese children with bacille Calmette–Guérin (BCG) multiple osteomyelitis with partial interferon (IFN)- γ receptor 1 (IFNGR1) deficiency. Heterozygous small deletions with frame shift (811 del4 and 818 del4) were detected, which were consistent with the diagnosis of partial dominant IFNGR1 deficiency. Case 1: a 2-year-old boy visited us because of limb and neck pain. He had been vaccinated with BCG at 17 months of age. Multiple destructive lesions were observed in the skull, ribs, femur, and vertebral bones. *Mycobacterium bovis* (BCG Tokyo 172 strain by RFLP technique) was detected in the bone specimen. The BCG multiple osteomyelitis was treated successfully without recurrence. Case 2: an 18-month-old girl developed multiple osteomyelitis 9 months after BCG inoculation. Radiologic images showed multiple osteolytic lesions in the skull, ribs, femur, and vertebrae. *M. bovis* (BCG Tokyo 172 strain) was detected in the cultures from a bone biopsy. Her clinical course showed recurrent osteomyelitis and lymphadenitis with no pulmonary involvement. The

effects of high-dose antimycobacterial drugs and IFN- γ administration were transient, and complete remission has since been achieved by combination antimycobacterial therapy, including levofloxacin. Partial dominant IFNGR1 deficiency is a rare disorder, but it should be considered when a patient presents with multiple osteomyelitis after BCG vaccination. The cases that are resistant to conventional regimens require additional second-line antituberculous drugs, such as levofloxacin.

Keywords Interferon- γ receptor 1 deficiency · Multiple osteomyelitis · Bacille Calmette–Guérin · Mycobacterial infection · Levofloxacin

Introduction

Interleukin-12 (IL-12)- and IFN- γ (IFNG)-mediated immunity plays an important role in host defense against intracellular pathogens [1]. Mendelian susceptibility to mycobacterial disease (MSMD) is a rare disorder and sometimes lethal disease that occurs in response to poorly virulent mycobacteria, such as bacille Calmette–Guérin (BCG) and environmental nontuberculous mycobacteria (NTM). In patients with MSMD, different types of mutations in six genes—IFNGR1, IFNGR2, IL12RB1, IL12B, STAT-1, and NEMO—have been revealed [2].

Sasaki et al. [3] previously reported a partial IFNGR1 mutation in three Japanese children with BCG osteomyelitis and in the father of one of the patients. We have followed the two unrelated cases over 10 years since their onset in the same department (Koshigaya Municipal Hospital). Based on our longitudinal experience, we intend to provide important clinical information for the diagnosis and treatment of IFN- γ RI deficiency in Japan.

K. Obinata · T. Lee · T. Niizuma · K. Kinoshita
Department of Pediatrics, Koshigaya Municipal Hospital,
Saitama, Japan

K. Obinata (✉)
Department of Pediatrics, Juntendo University Urayasu Hospital,
2-1-1 Tomioka, Urayasu, Chiba 279-0021, Japan
e-mail: obinata@juntendo-urayasu.jp

T. Shimizu
Department of Pediatrics, Faculty of Juntendo University,
Tokyo, Japan

T. Hoshina · Y. Sasaki · T. Hara
Department of Pediatrics, Graduate School of Medical Science,
Kyushu University, Fukuoka, Japan

Case report

Case 1

A Japanese boy became spontaneously positive to a tuberculin purified protein derivative (PPD) skin test at the age of 11 months. There was no family history of tuberculosis. A chest X-ray film showed no abnormal findings. The PPD skin test turned negative after 6 months of prophylactic treatment with isoniazid (INH). He was inoculated with BCG (Tokyo 172 strain) by the multiple puncture technique at the age of 17 months. Nine months later (at 26 months of age), he started to limp and could not move his neck. He visited Koshigaya Municipal Hospital, and multiple osteolytic lesions were observed on his skull, vertebrae (cervical and lumbar), ribs, and femur by X-ray, bone scintigram, and magnetic resonance (MR) imaging. *Mycobacterium* was detected in the bone biopsy. *Mycobacterium bovis* was identified as the BCG Tokyo 172 strain by restriction fragment length polymorphism (RFLP). The BCG osteomyelitis was treated successfully with antimycobacterial therapy with isoniazid (INH), rifampicin (RFP), and streptomycin (SM) for 1.5 years without recurrence. He is now 17 years old and has not had a mycobacterial infection since the treatment.

Case 2 (Fig. 1)

An 18-month-old girl (13 years old at present) developed left axillary lymphadenitis 2 months after BCG inoculation at the age of 8 months. Multiple skin eruptions and abscesses appeared 9 months after the vaccination. At the BCG inoculation site, there were signs of hypertrophic scar and keloid. Granuloma was also observed below the

inoculation site. X-ray, skeletal scintigram, and MR imaging showed multiple osteolytic lesions in the skull, ribs, femur, and vertebrae. A bone biopsy specimen of the femur revealed granulomatous inflammation without central necrosis. *M. bovis* (BCG Tokyo 172 strain) was detected in cultures from the bone biopsy by RFLP. She was treated with INH, RFP, and SM, and showed slow improvement. Eighteen months after her initial presentation, she started to develop recurrent osteomyelitis. Additional administration of ethambutol (EB) and IFN- γ was effective but the effect was temporary. She exhibited osteomyelitis soon after discontinuation of EB and RFP. High-dose INH and EB, with the addition of clarithromycin (CAM) and IFN- γ , proved effective. Her osteomyelitis appeared to have subsided. However, later, at the age of 11 years, she experienced a third relapse of the osteomyelitis. Antimycobacterial therapy was started again, but lymphadenitis also developed on her right supraclavicle. The findings from the swollen lymph nodes were nonspecific. Additional administration of high-dose IFN- γ was partially effective against the osteomyelitis and the lymphadenitis. As the cervical lymphadenopathy appeared again, the CAM was changed to levofloxacin (LVFX). A three-drug regimen of INH, RFP, and LVFX for a period of 9 months was successful in achieving remission.

The clinical features of these two unrelated Japanese children with BCG multiple osteomyelitis are summarized in Table 1. Two-color flow cytometric analysis was performed [3] and showed significantly higher levels of IFNGR1 expression on monocytes in both cases. IL-12 and IFN- γ production was normal. Genomic DNA was obtained from peripheral blood mononuclear cells. cDNA sequences were analyzed by polymerase chain reaction. Heterozygous small deletions with frame shift (case 1, 811 del4; case 2,

Fig. 1 Recurrent osteomyelitis and lymphadenitis in case 2. INH isoniazid, RFP rifampicin, SM streptomycin, EB ethambutol, CAM clarithromycin

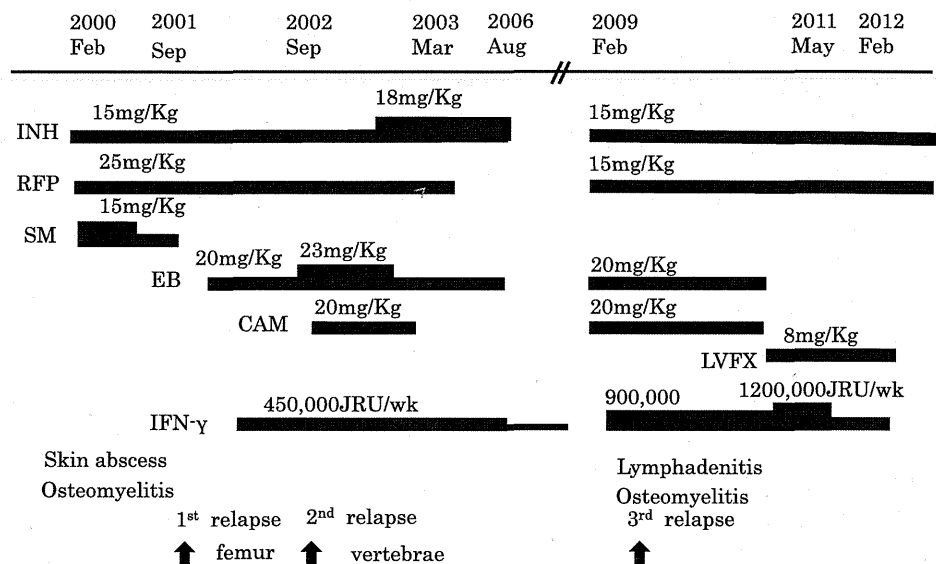


Table 1 Immunological data at the onset of patients with bacille Calmette–Guérin (BCG) osteomyelitis

| Case | 1 (17 years/M) | 2 (13 years/F) |
|--|------------------|---------------------|
| BCG given at | 1 year 5 months | 8 months |
| Age at onset | 2 years 2 months | 1 year 5 months |
| Type | Multiple | Multiple, recurrent |
| Histology | Inflammation | Granuloma |
| Other organs | None | Skin, lymph node |
| WBCs/ μ l | 5,300 | 29,600 |
| Lymphocytes/ μ l | 3,657 | 7,400 |
| IgG, mg/dl | 1,370 | 1,430 |
| IgA, mg/dl | 188 | 104 |
| IgM, mg/dl | 602 | 181 |
| CD3 cells, % | 40.7 | 56.6 |
| CD4:CD8 | 3 | 3 |
| CD19 cells, % | 10.4 | 26.4 |
| PHA response | Normal | Normal |
| Cytokine production IL-12/INF- γ | Normal | Normal |

818 del4) were detected, which were consistent with the diagnosis of partial dominant IFNGR1 deficiency (data not shown). Sequence analysis of six coding regions was performed and showed that none of the family members of the patients had any mutations. Furthermore, neither sets of parents were consanguineous. Thus, de novo mutation had occurred in both cases 1 and 2.

Discussion

Bacille Calmette–Guérin vaccines are safe in immunocompetent hosts, and Japanese BCG substrain Tokyo 172 is the safest BCG in the world [4]. Complications of BCG vaccination can be severe and life threatening in infants with immunodeficiency. Systemic adverse reactions to BCG vaccine, including osteomyelitis and disseminated BCG infection, are rare. Toida and Nakata [5] reviewed severe adverse reactions to BCG from 1951 to 2004 in Japan and identified 39 cases (incidence rate, 0.0182 cases per 100,000 vaccinations). Thirteen cases exhibited primary immunodeficiency; 5 of these exhibited chronic granulomatous diseases, 4 exhibited severe combined immunodeficiency, and 4 exhibited IFNGR1 deficiency. Unidentified defects in cellular immunity were observed in 6 cases. The 6 fatal cases had cellular immunodeficiencies. Bone and joint involvement was observed in 27 cases, 15 cases with multiple lesions and 12 cases with single site lesions.

Hoshina et al. [6] analyzed the clinical characteristics and the genetic background of 46 patients with MSMD in

Japan from 1999 to 2009, and found that 6 had mutations in the IFN- γ R1 gene. All the cases of IFN- γ R1 deficiency exhibited multiple osteomyelitis, and disseminated mycobacterial infection recurred in 5 patients. All the patients exhibited the partial dominant type, and 4 of them had 818 del4. Two of the patients were from the same family, and therefore autosomal dominant inheritance was suspected. The 4 others were considered to have occurred spontaneously. In Taiwan, 3 patients from two unrelated families were identified with a hotspot IFNGR1 deletion mutation (818 del4) and exhibited chronic granulomatous disease-like features, presenting as cutaneous granuloma and multiple osteomyelitis infected with NTM [7]. Fewer patients of Asian origin have been reported with partial dominant IFNGR1 deficiency compared with those of Western countries [8]. The clinical phenotype of partial dominant IFNGR1 deficiency is milder than that of complete deficiency. In this type, BCG and NTM are the major pathogens. Complete IFN- γ receptor deficiency is associated with the early onset of severe disease caused by BCG or NTM, whereas the other genetic forms are associated with a milder course of mycobacterial infection [8].

Patients with partial IFGR1 deficiency usually respond well to antibiotic treatment, and for those who do not respond well, additional IFN- γ therapy has been shown to be effective [9]. There is no single standard regimen for the treatment of children with BCG osteomyelitis. *M. bovis* is resistant to pyrazinamides because of the expression of a pyrazinamidase. Case 1 was successfully treated with a long-term combination therapy of INH, RFP, and SM. However, in case 2, conventional therapy was inadequate to fight the infection. Additional administration of EB and relatively low dose IFN- γ was not able to control the intractable osteomyelitis. As NTM infection was also possible, high-dose EB, INH, and CAM were administered. The regimen was effective but temporary. Combination therapy, including LVFX and high-dose INF- γ , was the most successful strategy. Treatment with second-line antituberculous drugs, such as fluoroquinolone, and two first-line drugs (RFP and EB), may be more effective than RFP and EB alone against multidrug-resistant *M. bovis* [10]. LVFX plays an important role as a substitute agent for those patients who are intolerant of first-line antituberculous agents.

IFN- γ receptor deficiency is a rare disorder that should be considered when patients exhibit BCG lymphadenitis and disseminated osteomyelitis. Multifocal mycobacterial osteomyelitis without other organ involvement is only seen in dominant partial IFNGR1 deficiency [6, 8]. This type of immunodeficiency tends to exhibit recurrent mycobacterial infection and resistance to conventional antimycobacterial therapy. LVFX is likely an effective option for cases with the partial dominant type that are resistant.